Footprints of New Physics in the Angular Distribution of Flavour Changing Charged Current Decay $B_s^0 \to K_1(1270)(\to \rho(770)\pi)l\bar{\nu}_l$

By

Mahira Tooba

0000365380

MS Physics 2021

Supervisor

Dr. Muhammad Ali Paracha

Department of Physics

School of Natural Sciences (SNS)

National University of Sciences and Technology (NUST)

Islamabad, Pakistan

May 2024

Footprints of New Physics in the Angular Distribution of Flavour Changing Charged Current Decay $B_s^0 \to K_1(1270)(\to \rho(770)\pi)l\bar{\nu}_l$

By

Mahira Tooba

00000365830

Supervisor

Dr. Muhammad Ali Paracha

———————————

A thesis submitted in conformity with the requirements for

the degree of *Master of Science* in

Physics

Department of Physics

School of Natural Sciences (SNS)

National University of Sciences and Technology (NUST)

Islamabad, Pakistan

May 2024

THESIS ACCEPTANCE CERTIFICATE

Certified that final copy of MS thesis written by **Mahira Tooba** (Registration No. **00000365380**), of **School of Natural Sciences** has been vetted by undersigned, found complete in all respects as per NUST statutes/regulations, is free of plagiarism, errors, and mistakes and is accepted as partial fulfillment for award of MS/M.Phil degree. It is further certified that necessary amendments as pointed out by GEC members and external examiner of the scholar have also been incorporated in the said thesis.

Signature: _____

Name of Supervisor: Dr. Muhammad Ali Paracha

Date: _____30-4-2024_____

Signature (HoD): _____

Date: _____30-4-2024_____

Signature (Dean/Principal): _____

Date: _____06.05.2024_____

National University of Sciences & Technology

MS THESIS WORK

We hereby recommend that the dissertation prepared under our supervision by: **"Mahira Tooba"** Regn No. **00000365380** Titled: **"Footprints of New Physics in the Angular Distribution of Flavour Changing Charged Current Decay B0s → K1(1270)(→ρ(770)π)l ⁻ νl"** accepted in partial fulfillment of the requirements for the award of **MS** degree.

Examination Committee Members

1. Name: DR. SAADI ISHAQ   Signature: _____

2. Name: DR. FAISAL MUNIR BHUTTA   Signature: _____

Supervisor's Name: DR. MUHAMMAD ALI PARACHA   Signature: _____

_____   02-04-2024
Head of Department   Date

COUNTERSINGED

Date: 06-05-2024   _____
                                     Dean/Principal

This thesis is dedicated to *my beloved parents*, the tireless pillars of my journey, whose relentless support and unwavering belief have been the bedrock of my motivation and success. Their boundless encouragement and sacrifices stand as a testament to the immeasurable strength and guidance they've provided throughout my academic pursuits and beyond.

Abstract

The New Physics effects observed through the anomalies in the b $\rightarrow cl\bar{\nu}_l$ decay processes serve as an insight to look for the possibility of utilizing the observables inferred from the detailed angular analysis of b $\rightarrow ul\bar{\nu}_l$ decay at the quark level. A full differential angular distribution of the four-fold Footprints of New Physics in the Angular Distribution of Flavour Changing Charged Current Decay $B_s^0 \rightarrow K_1(1270)(\rightarrow\rho(770)\pi)l\bar{\nu}_l$ decay has been analyzed within the Standard Model and also in the model-independent framework. The detailed investigation of above mentioned Flavour Changing Charged Current process has been done to investigate the Physics Beyond the Standard Model. For this very semileptonic decay channel, multiple q^2 dependent physical observables along with a special focus on parallel angular coefficient functions have been calculated. Results, thus obtained, exhibit sensitivity of these observables to the NP Wilson Coefficients. Future experimental prospects would be enlightening for this kind of decay to unfold the underlying complete structure of NP from the quark flavour sector.

Keywords: *Flavour Changing Charged Current, semileptonic, cascade decay*

Acknowledgments

Contents

List of Figures

List of Tables

List of Abbreviations and Symbols

Abbreviations

NP   New Physics

SM   Standard Model

BSM   Beyond Standard Model

FCCC   Flavour Changing Charged Current

FCNC   Flavour Changing Neutral Current

EFT   Effective Field Theory

NLO   Next to Leading Order

QCD   Quantum Chromodynamics

BR   Branching Ratio

FBA   Forward Backward Asymmetry

QFT   Quantum Field Theory

VEV   Vacuum Expectation Value

EM   Electromagnetic

SSB   Spontaneous Symmetry Breaking

Introduction

J.J Thompson's discovery of electron in 1887 gave a new direction of thinking to mankind who was previously considering an atom to be the ultimate constituent of matter. Eversince then the Rutherford's discovery of proton in 1911, Carl Anderson's discovery of positron and James Chadwick's discovery of neutron in 1932 alongside many more particles keep on broadening the picture and a new term tossed by the physicists, came on the forefront known as "Particle Physics". The urge of uncovering the ultimate structure of the universe and to discover it at the smallest possible level has lead to the formulation of what we call the Periodic Table of particles; The Standard Model of Particle Physics.

Particle physics, at its core, is a captivating scientific field that delves into the fundamental constituents of the universe and the forces that govern their interactions. It is a quest to understand the tiniest building blocks of matter and the essential rules that dictate their behavior. In this introductory exploration of particle physics, we embark on a journey into the realm of subatomic particles, shedding light on the intriguing anomalies and challenges that have perplexed physicists for decades.

One of the most intriguing aspects of particle physics is the presence of anomalies—peculiar observations and phenomena that defy the well-established theoretical framework known as the Standard Model. These anomalies, though rare and elusive, have the potential to revolutionize our understanding of the universe. Some anomalies hint at the existence of new, undiscovered particles or interactions, pushing scientists to explore beyond the boundaries of what is currently known.

As we venture deeper into the world of particle physics, we encounter some of its most profound mysteries and challenges. The hierarchy problem, for instance, raises ques-

tions about the vast disparity between the strength of gravity and the other fundamental forces, a puzzle that remains unsolved. Furthermore, the mystery of the universe's dominance by matter over antimatter continues to baffle researchers, as the Standard Model offers no definitive explanation for this cosmic inequality. These enigmatic questions, among others, drive the relentless pursuit of knowledge in particle physics and underscore the boundless curiosity of humanity as we strive to unravel the secrets of the subatomic world.

This significant formulation incorporates three out of four fundamental forces. This group theoretical, quantum mechanical portrayal of particles is complete in many senses yet carries some unanswered questions [4]. The shortfall starts from the exclusion of a renormalizable quantum theory for gravitational interaction and extends to

(i) why there are only 3 generations of leptons and quarks? (distinctly separated in light to heavy families)

(ii) why does this mass hierarchy exist? (the experimentally observed mass value of the Higgs boson shows quite a large discrepancy from its predicted value in the SM; the Higgs mechanism doesn't specify the absolute masses of particles but elucidates how they acquire mass.).

(iii) absence of candidate particles for dark matter and the puzzle of dark energy.

(iv) inequality in the existence of observed matter and antimatter whereas the Big Bang predicted them to be in equal proportions (CP violation).

(v) the massless neutrinos predicted by the SM have experimentally measured non-zero mass values.

The limitations listed above diverge the attention of SM to the necessity of the use of approaches beyond SM [5]. This quest of searching for novelty represents highly esteemed investigative research in Particle Physics these days.

One of the profound areas for the novel searches is B-Physics, so fundamentally important that CERN has dedicated a whole sector; LHCb for the searches of B-meson decays and related bottom quark containing species. These particles are ideal probes for potential exploration of deviations from currently known physics due to their unique decay patterns and sensitivity to subtle quantum effects. Any observed deviations or inconsistencies in these measurements could hint at the existence of new particles or

interactions that lie beyond the scope of the Standard Model, offering a window into understanding physics that extends beyond our present understanding.

Much work has been done in the field by taking up different kinds of toy models i.e. leptoquark, Z-prime, composite and other models. One of the possible approaches is to work in a model-independent scenario. This thesis is based on the aforementioned technique thereby extending the SM from its V-A structure to the incorporation of S-P and T-T5 structures.

The $B_s^0 \rightarrow K_1(1270)(\rightarrow\rho(770)\pi)l\bar{\nu}_l$ cascade decay has been studied in the helicity framework. The angular coefficients for the longitudinal polarization of ρ have been calculated. Based on these coefficients other physical observables are also calculated. Chapter 2 is a complete highlight of the SM involving the lagrangian, SSB, Flavour Physics and CKM matrix. A discussion of NP emerging by the involvement of EFT at the electroweak scale is included in next part. Chapter 4 deals with the theoretical framework of the above-mentioned decay. The analysis of results is discussed in Chapter 5. Finally, the last chapter concludes our research.

The Standard Model of Particle Physics

A keen inspection of fundamental building blocks of nature and their mutual interactions has led to the formulation of the SM of matter particles and intermediate ones. Its a gauge theory with the underlying symmetry group $SU(3)_C \times SU(2)_L \times U(1)_Y$. The subscripts correspond to physical applications i.e. C refers to strong charge (colour), L tells about the left-handedness of the SU(2) group and Y is the quantum number for weak hypercharge. This group theoretical, quantum mechanical approach encompasses three out of four fundamental forces with the exclusion of gravity. The following sections include a complete overview of the particles included in the SM and their properties. The section ahead deals with the Lagrangian of SM along with a discussion on SSB and Higgs mechanism. Lastly, the final section discusses Flavour Physics and CKM Matrix.

2.1   Overview of Standard Model

All the matter content present in the universe interacts through four fundamental forces known to date. For a complete understanding of the structure of the universe, we should know its structure first at the fundamental level. The SM describes the properties and characteristics of these building blocks. SU(3) group deals with quantum chromodynamics and the $SU(2) \times U(1)$ describes the electro-weak part of the SM.

2.1.1 The Elementary Particles and Forces

The SM illustrates all the particles of which matter is composed. The negatively charged electrons, positively charged protons and neutral neutrons are the ultimate constituents of matter. Electrons are entities that can exist independently and are fundamental particles whereas protons and neutrons are composite particles and exist as a combination of quarks. Quarks can not exist independently and are always found in the combination of three quark states as baryons and/or a quark and an anti-quark combined state known as meson. Baryons and mesons collectively form the confined states of quarks called hadrons. There are three generations of quarks and leptons. The first family of quarks contains up and down quarks; protons is a combination of two up quarks and one down quark, neutron is formed from two down and one up quark. The second generation includes charm and strange quarks and the third family contains top and bottom quarks. All these three families of quarks carry colour charges; red, green, blue, electric charges and masses. They interact via strong, electromagnetic, gravitational and weak interactions. The third generation being the heaviest and the first generation is the lightest one. Tables 2.1 and 2.2 drawn below contain the details of all 6 quarks and 6 leptons included in SM [6].

Quarks			
Family	Particle	Charge	Mass (GeV)
First	up(u)	+2/3	0.005
	down(d)	-1/3	0.003
Second	charm(c)	+2/3	1.3
	strange(s)	-1/3	0.1
Third	top(t)	+2/3	174
	bottom(b)	-1/3	4.5

Table 2.1: Table 2.1: The six fundamental quarks

Leptons are particles that do not carry a strong charge and are therefore colourblind. They interact through all three forces except the strong force. The lepton neutrinos interact via weak forces only. All these leptons and quarks are fermions; spin-1/2 particles.

Apart from these 12 fundamental fermions, there are gauge bosons in the SM which

Leptons			
Family	Particle	Charge	Mass (GeV)
First	electron(e)	-1	0.0005
	electron neutrino(ν_e)	0	$< 10^{-9}$
Second	muon(μ)	-1	0.106
	muon neutrino(ν_μ)	0	$< 10^{-9}$
Third	tau(τ)	-1	1.78
	tau neutrino(ν_τ)	0	$< 10^{-9}$

Table 2.2: Table 2.2: The six fundamental leptons

are the force carriers and are responsible for the interactions between particles. Among these; photons are responsible for all electromagnetic interactions, strong force is mediated by gluons and weak nuclear force is mediated via charged W^+, W^- and neutral Z^0. From these vector bosons, photons and gluons are massless. Considering the group structure, the SU(3) group has 8 generators and in the strong interactions, 8 gluons arise naturally. For the electroweak group $SU(2) \times U(1)$ there are 3+1 generators corresponding to 3 weak mediators and a photon. The force carriers with their relative strengths are shown in the table [7] below.

Force	Strength	Boson	Spin	Mass (GeV)
Strong	1	Gluon	1	0
Electromagnetism	10^{-3}	Photon (γ)	1	0
Weak	10^{-8}	W Bosons (W$^+, W^-$)	1	80.4
	10^{-8}	Z Boson (Z^0)	1	91.2
Gravity	10^{-37}	Graviton (hypothetical)	2	0

Table 2.3: The known four forces, their carriers and relative strengths of force carriers at a distance of one fermi

Graviton is a proposed candidate for the gravitational interactions and is yet to be discovered. Another boson of spin zero included in the SM is the Higgs boson. Its mass is 125 GeV. This is the particle responsible for assigning masses to all particles through the well-known Higgs Mechanism. SM is a well-tested theory and proved to be completely in agreement with the experimentation.

In terms of QFT, particles are nothing but the quantized excitations of the underlying fields. For the case of strong and electromagnetic interactions, the vacuum expectation values of such fields are zero and also for the fields corresponding to the fundamental fermions. The VEV for the Higgs field is believed to be non-zero. The masses of weak gauge bosons W^+, W^- and Z^0 have a close correspondence with Higgs boson mass of the order of 100 Gev and this energy scale is said to be an electroweak scale.

2.1.2 The Standard Model Vertices

In the Standard Model of particle physics, the interactions between fermions (such as quarks and leptons) and gauge bosons (like photons, gluons, W and Z bosons) are characterized by specific vertices. These vertices illustrate the relationships among these particles during interactions.

The nature of these interactions is dictated by both the properties of the gauge bosons involved and how the bosons interact with fermions. For instance, the three-point vertex, which involves a gauge boson and an incoming as well as an outgoing fermion, serves as a visual representation of their interaction dynamics. These interactions are described through various diagrams denoted by figures (2.1 - 2.4).

Each type of interaction at these vertices is associated with a coupling strength represented by the symbol "g." This coupling strength, g, is a fundamental parameter that characterizes the strength of the interaction between the fermions and the gauge bosons involved in the process.

Strong Force

The strong force operates uniquely among quarks due to their possession of a distinctive attribute known as the color charge within the framework of QCD. This force maintains the constancy of quark flavors during interactions. In the realm of strong interactions, the strong coupling constant, a dimensionless parameter, dictates the behavior of this force, and its characteristics vary with differing energy scales. At lower energy levels, the strong coupling constant reflects a considerable intensity, depicting robust interactions between quarks. Conversely, at higher energy levels, this constant diminishes, indicating reduced interactions among quarks. The inherent potency of the QCD interaction, often denoted as g_s corresponds to 1, significantly surpasses the strengths of other fundamental forces. This highlights the supremacy of the strong force among these forces, particularly
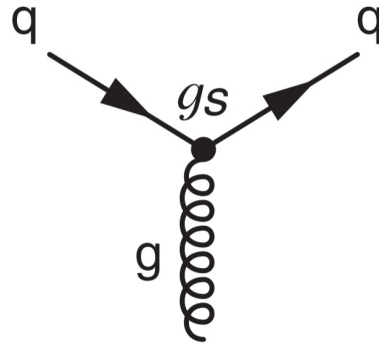
Figure 2.1: Strong interaction vertex
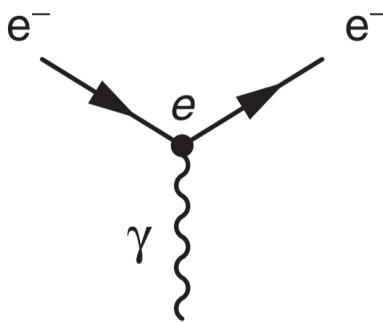
Figure 2.2: EM interaction vertex

in contexts relevant to nuclear physics. See 2.1

Electromagnetic Force

The electromagnetic force affects all charged particles, creating a mutual influence between them. In interactions governed by electromagnetism, there is no alteration in particle flavor. Such interactions involve an exchange of a photon between the charged particles. The fine structure constant serves as a parameter that precisely measures the strength of the electromagnetic force. All interactions occurring at the Newtonian scale are governed by this force. The strength of the fine structure constant e is of the order 1/137 [7]. See Fig: 2.2

Weak Force

Weak force differs from EW and strong interactions in many ways. All twelve fermions can interact weakly as they all contain weak isospin. Weak interactions involve two kinds; one in which the interaction occurs among the same flavors of leptons and the other in which different flavors are involved.
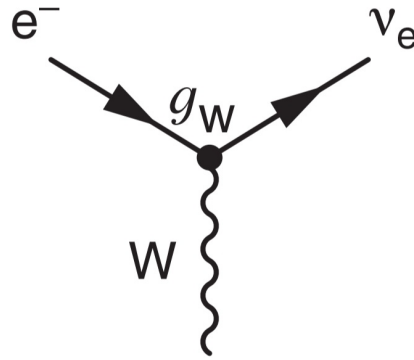
Figure 2.3: Weak charged current vertex
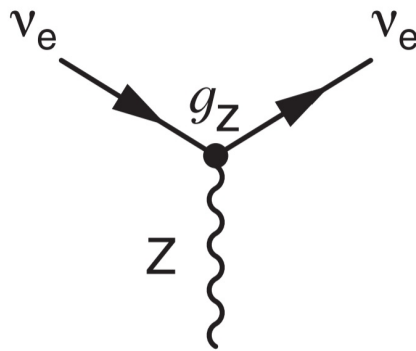
Figure 2.4: Weak neutral current vertex

Weak Charged Current Interaction

These are the weak interactions carried by W^+ and W^-. Fermions connected through such interactions have a disparity of one unit charge. It stands as the sole interaction capable of altering particle flavors. Specifically for leptons, such interaction connects a lepton to the corresponding lepton-neutrino. At quark level a $b \rightarrow$ u transition is an example of this type of interaction. Such a decay is the subject of this work. The vertex interaction strength g_W of the order 1/30 [7] is shown in 2.3.

Weak Neutral Current Interaction

These are the weak interactions carried by Z^0. Fermions connected through such interactions may interact via photon and involve change in particle flavors. These interactions involve no change of charge . Within SM such decays occur at loop level involving GIM mechanism. The vertex interaction strength g_Z of the order 1/30 [7] is shown in 2.4.

2.2 Standard Model Lagrangian

The Lagrangian density for the SM is written as

$$\mathcal{L}_{SM} = \mathcal{L}_G + \mathcal{L}_F + \mathcal{L}_H + \mathcal{L}_Y \tag{2.2.1}$$

SM is a non-abelian gauge theory that involves certain renormalizations. The Lagrangian of the Standard Model in particle physics is a mathematical formulation that describes the dynamics and interactions of fundamental particles and their associated fields. Its a sum of various terms, each representing different interactions and particle properties. Breaking down the Standard Model Lagrangian term by term involves dissecting its components, starting from $\mathcal{L}_G$ which corresponds to the gauge bosons. The terms involved in $\mathcal{L}_G$ describe the kinetic energy of the gauge bosons (photon, W's and Z bosons and gluons) and the way through which interact with the corresponding gauge fields. Each of the gauge boson has its own kinetic term, which typically involves derivatives of the gauge fields [6].

$$\mathcal{L}_G = -\frac{1}{4} G^j_{\mu\nu} G^{j\mu\nu} - \frac{1}{4} W^j_{\mu\nu} W^{j\mu\nu} - \frac{1}{4} B_{\mu\nu} B^{\mu\nu} \tag{2.2.2}$$

where $G^j_{\mu\nu}, W^j_{\mu\nu}$ and $B_{\mu\nu}$ are field strength tensors respectively for $SU(3)_C$ colour symmetry , $SU(2)_L$ weak isospin and $U(1)_Y$ weak hypercharge. The three and four-point self-interaction terms for $G^j_{\mu\nu}$, $W^j_{\mu\nu}$ are also included as they have quadratic terms in their gauge fields as $SU(3)_C$ and $SU(2)_L$ are non-abelian. $U(1)_Y$ is an abelian gauge group so it does not involve self-interaction.

Therefore, $G^j_{\mu\nu} = \partial_\mu \mathrm{G}^j_\nu - \partial_\nu \mathrm{G}^j_\mu - g_s f_{jkl} G^k_\mu G^l_\nu$ such that $j, k, l = 1 \ldots 8$ for strong interactions

$W^j_{\mu\nu} = \partial_\mu \mathrm{W}^j_\nu - \partial_\nu \mathrm{W}^j_\mu - g_w \epsilon_{jkl} W^k_\mu W^l_\nu$ such that $j, k, l = 1 \ldots 3$ for weak interactions

and

$B_{\mu\nu} = \partial_\mu \mathrm{B}_\nu - \partial_\nu \mathrm{B}_\mu$ for EM interactions

where g_w and g_s are the gauge couplings and f_{jkl} and ϵ_{jkl} are the representation for the structure constants.

$\mathcal{L}_F$ includes all the matter particles; all fermions present in the SM. The 3 generations of leptons and quarks; their kinetic energies, interaction terms and associated derivatives are the consistency of $\mathcal{L}_F$. Each generation comprises of

L-doublets:

$$q_{mL}^0 = \begin{pmatrix} u_m^0 \\ d_m^0 \end{pmatrix}_L, l_{mL}^0 = \begin{pmatrix} \nu_m^0 \\ e_m^0 \end{pmatrix}_L \qquad (2.2.3)$$

R-singlets:

$$u_{mR}^0, d_{mR}^0, \nu_{mR}^0, e_{mR}^0 \qquad (2.2.4)$$

where L-fields are SU(2) doublets and R-chiral fields are SU(2) singlets. These fields, as referred to by superscript 0, are weak eigenstates with definite transformation properties. Here m=1,2,3 correspond to three families of quarks and leptons. The chiral representation of $SU(2)_L$ and $U(1)_Y$ is used and yet no mass term is involved. The fermionic Lagrangian involving only the kinetic energy terms and derivatives is written as

$$\mathcal{L}_F = \sum_{m=1}^{3} (\bar{q}_{mL}^0 \iota \slashed{D}^\mu q_{mL}^0 + \bar{l}_{mL}^0 \iota \slashed{D}^\mu l_{mL}^0 + \bar{u}_{mR}^0 \iota \slashed{D}^\mu u_{mR}^0)$$

$+\sum_{m=1}^{3} (\bar{d}_{mR}^0 \iota \slashed{D}^\mu d_{mR}^0 + \bar{e}_{mR}^0 \iota \slashed{D}^\mu e_{mR}^0 + \bar{\nu}_{mR}^0 \iota \slashed{D}^\mu \nu_{mR}^0)(2.2.5)$

The Lagrangian density for Higgs sector $\mathcal{L}_H$ is written as

$$\mathcal{L}_H = (D^\mu \phi)^\dagger (D_\mu \phi) - V(\phi) \qquad (2.2.6)$$

where ϕ is the complex scalar

$$\phi = \begin{pmatrix} \phi^+ \\ \phi^0 \end{pmatrix} \qquad (2.2.7)$$

and the covariant derivative for this case would be written exactly similar to that of $\mathcal{L}_F$. Its

$$D_\mu \phi = (\partial_\mu + \frac{\iota g}{2} \tau.W_\mu + \frac{\iota g'}{2} \tau.B_\mu) \qquad (2.2.8)$$

The Higgs potential is written as

$$V(\phi) = \mu^2 \phi^\dagger \phi + \lambda (\phi^\dagger \phi)^2 \qquad (2.2.9)$$

considering $SU(2) \times U(1)$ invariance whereas $\phi^\dagger \phi = \phi^- \phi^+ + \phi^{0\dagger} \phi^0$. For the vacuum stability, $\lambda > 0$ is required which can give two possibilities for the ground state.

(i) If $\mu^2 > 0$, the minima of Higgs potential is at $\phi = 0$. This provides a parabolic-shaped curve for the potential showing how the mass of massive particles varies with μ.

11
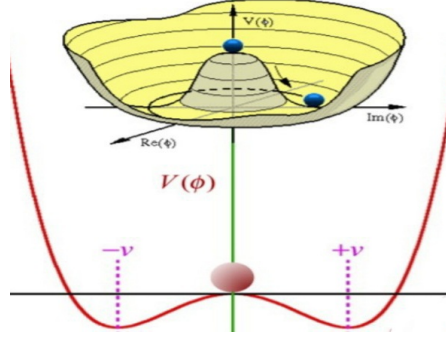
Figure 2.5: Mexican hat Potential [1]

(ii) If $\mu^2 < 0$, we obtain a Mexican hat-shaped curve as a result of SSB. The curve as shown in 2.5 represents that the minima is non-zero and the curve has shifted below the zero. As the VEV is non-zero, it spontaneously breaks the electroweak guage symmetry result the Higgs Mechanism; through which bosons interact with Higgs field and obtain their masses. The minima occurs at $\phi = \sqrt{\frac{-\mu^2}{\lambda}}$

$\mathcal{L}_Y$ is the part which contains the mass terms. After SSB, the scalar (Higgs) field interacts with Dirac field, as a result, fermions get masses. The $SU(2) \times U(1)$ symmetry breaking provides the masses to quarks and leptons through Yukawa couplings. The corresponding lagrangian part is written as

$$\mathcal{L}_Y = \sum_{m,n=1}^{3} (\Gamma^u_{mn} \bar{q}^0_{mL} \tilde{\phi} u^0_{nR} + \Gamma^d_{mn} \bar{q}^0_{mL} \phi d^0_{nR} + \Gamma^e_{mn} \bar{l}^0_{mL} \phi e^0_{nR} + \Gamma^\nu_{mn} \bar{l}^0_{mL} \tilde{\phi} \nu^0_{nR}) + h.c$$

$$(2.2.10)$$

where

$$\phi = \begin{pmatrix} \phi^+ \\ \phi^0 \end{pmatrix}, \qquad\qquad \tilde{\phi} = \begin{pmatrix} \phi^{0\dagger} \\ -\phi^- \end{pmatrix}$$

are Higgs doublet and its conjugate respectively. $\Gamma^u, \Gamma^d, \Gamma^e, \Gamma^\nu$ are $F \times F$ arbitrary matrices which determine fermion masses and mixings; through which free parameters are added.

As a fine analogy, one can think of SSB in a way that there was an atom, with multiple degenerate ground states, is excited. It could attain a multitude of states upon de-excitation. Once it has chosen a specific state to get de-excited, at that very moment the symmetry is broken and a specific choice of state has been made.

2.3   Flavour Physics and CKM Matrix

Flavour Physics is the physics of interactions that distinguish among *flavours*. Neither strong nor EM can distinguish between flavours. In SU(3) triplet representation, we say, (u,c,t) are three flavours of up quark with +2/3 charge and (d,s,b) as three flavours of down quark with -1/3 charge. (e, μ, τ) are three flavours of charged leptons with -1 charge and $(\nu_e, \nu_\mu, \nu_\tau)$ are 3 flavours of neutral leptons and are singlets of $SU(3)_c$. Photons and gluons are flavour blind. What distinguishes among flavours is W^+, W^- and also the Yukawa interactions.

The CKM (Cabibbo-Kobayashi-Maskawa) matrix is pivotal in the Standard Model of particle physics, as it explains the flavor transition by allowing the mixing of quark flavor in weak interaction (flavour dynamics).CKM matrix gives an insight for CP violation. CP violation involves a breach in combined charge conjugation (C) and parity (P) symmetry in specific particle interactions, crucial for understanding matter dominance. Through experimental observation, its vivid that complex phases within the CKM matrix are allowed for CP violation in weak interactions.

Observations of quark transitions, especially those involving B mesons and kaons are expanded by CKM matrix. The CKM matrix links weak interaction eigenstates of quarks (quark flavor states) to their mass eigenstates. Its a unitary matrix with complex numbers, indicating coupling strength and relative phase between different quark flavors.

$$V_{CKM} = \begin{pmatrix} V_{ud} & V_{us} & V_{ub} \\ V_{cd} & V_{cs} & V_{cb} \\ V_{td} & V_{ts} & V_{tb} \end{pmatrix} \tag{2.3.1}$$

It is important to mention that V_{CKM} is unitary such that $V_q^\dagger V_q = V_q V_q^\dagger = I$, where q could be any of the six flavours. The matrix elements describe the probability amplitudes for a quark of one flavor to transition into another during weak interactions.

CKM matrix relate mass (physical) eigenbases to weak eigenbases as follows

$$\begin{pmatrix} d' \\ s' \\ b' \end{pmatrix} = V_{CKM} \begin{pmatrix} d \\ s \\ b \end{pmatrix} \tag{2.3.2}$$

Various parameterizations exist for the 3×3 CKM matrix. One parameterization, called the standard parametrization, is constructed via the multiplication of three rotation matrices. Another parameterization, known as the Wolfenstein parameterization, specifically addresses and clarifies the off-diagonal elements of the matrix.

2.3.1 Standard Parametrization

As stated earlier standard parameterization is obtained by taking the product of three of three rotation matrices. We have, therefore,

$$V_{CKM} = \begin{pmatrix} V_{ud} & V_{us} & V_{ub} \\ V_{cd} & V_{cs} & V_{cb} \\ V_{td} & V_{ts} & V_{tb} \end{pmatrix} = \begin{pmatrix} 1 & 0 & 0 \\ 0 & c_{23} & s_{23} \\ 0 & -s_{23} & c_{23} \end{pmatrix} \begin{pmatrix} c_{13} & 0 & s_{13}e^{-\iota\delta} \\ 0 & 1 & 0 \\ -s_{13}e^{\iota\delta} & 0 & c_{13} \end{pmatrix} \begin{pmatrix} c_{12} & s_{12} & 0 \\ -s_{12} & c_{12} & 0 \\ 0 & 0 & 1 \end{pmatrix}$$

$$= \begin{pmatrix} c_{12}c_{13} & s_{12}c_{13} & s_{13}e^{-\iota\delta} \\ -s_{12}c_{23} - c_{12}s_{23}s_{13}e^{\iota\delta} & c_{12}c_{23} - s_{12}s_{23}s_{13}e^{\iota\delta} & s_{23}c_{13} \\ s_{12}s_{23} - c_{12}c_{23}s_{13}e^{\iota\delta} & -c_{12}s_{23} - s_{12}c_{23}s_{13}e^{\iota\delta} & c_{23}c_{13} \end{pmatrix} \quad (2.3.3)$$

where $c_{ij} = \cos\theta_{ij}$ and $s_{ij} = \sin\theta_{ij}$, θ_{12}, θ_{13} and θ_{23} are real mixing angles and δ is the CP-violating phase or Kobayashi-Maskawa phase [7].

2.3.2 Wolfenstein Parametrization

The Wolfenstein parametrization to $O(\lambda^4)$ is given as

$$V_{CKM} = \begin{pmatrix} 1 - \lambda^2/2 & \lambda & A\lambda^3(\rho - \iota\eta) \\ -\lambda & 1 - \lambda^2/2 & A\lambda^2 \\ A\lambda^3(1 - \rho - \iota\eta) & -A\lambda^2 & 1 \end{pmatrix} \quad (2.3.4)$$

such that $\lambda = |V_{us}|$ whereas $s_{13} << s_{23} << s_{12}$. Here four mixing parameters are involved. λ is the expansion parameter, η is CP violating phase. Beside λ, the three parameters are $O(1)$. Thus from the unitarity condition, we have weak universality testing for the diagonal elements,

$$(V_q V_q^\dagger)_{11} = |V_{ud}^2| + |V_{us}|^2 + |V_{ub}|^2 = 1$$
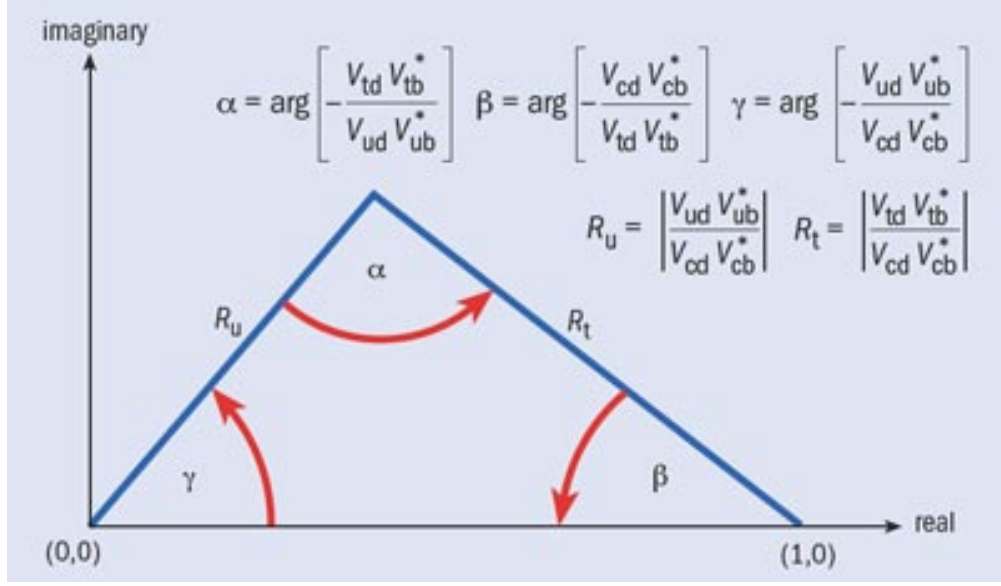
Figure 2.6: The unitarity triangle showing angles and relations between CKM matrix elements [2]

For the off-diagonal elements,

$$(V_q^\dagger V_q)_{31} = V_{ub}^* V_{ud} + V_{cb}^* V_{cd} + V_{tb}^* V_{td} = 0$$

A total of six equations like the above can be written. These relations are visually depicted as triangles called 'Unitarity triangles' within the complex plane, providing a geometric representation. All six triangles have similar areas. The length of two complex sides and three angles are explicitly mentioned in the Fig: 2.6

The current status of Wolfenstein parameters is

$$A = 0.790^{+0.017}_{-0.012}, \lambda = 0.22650^{+0.00048}_{-0.00048}, \bar{\rho} = 0.141^{+0.016}_{-0.017}, \bar{\eta} = 0.3571^{+0.011}_{-0.011}$$

where $\bar{\rho} = \rho(1 - \lambda^2/2)$, $\bar{\eta} = \eta(1 - \lambda^2/2)$. The phases of the unitarity triangle are also well determined. Direct and indirect measurements of angles are in well agreement [8].

$$\alpha = [91.7^{+1.7}_{-1.1}]^\circ, \beta = [22.56^{+0.47}_{-0.40}]^\circ, \gamma = [65.8^{+0.94}_{-1.29}]^\circ$$

2.3.3 Charged and Neutral Currents

Keeping CKM matrix in view; the interactions which alter both flavour and charge are called flavour-changing charged current (FCCC) interactions and are mediated by charged weak guage bosons. FCCC occur at tree level in SM. On the other hand if Z^0

(primarily) or γ (as in some super-symmetric or other extensions) is the weak mediator, then flavour will be altered but not the charge and such interactions are called flavour-changing neutral current (FCNC) interactions. FCNC occur at loop level in SM by the well-known GIM mechanism [9].

2.4   Looking Ahead from Standard Model

The realms where SM falls short, searches for Physics BSM come on the forefront. One of the prevalent approaches is Grand Unified Theories (GUTs) which aims to unify three fundamental forces into a single force at very high energies. These theories seek to explain aspects unaccounted for by the SM, such as the quantization of charge and the unification of forces.

Another possibility is to work with Effective Field Theories (EFTs). This approach proposes modifications or extensions within the framework of the SM to address its limitations, often at lower energy scales. EFTs provide a simplified description of high-energy phenomena, allowing physicists to probe beyond known boundaries without needing a full theory. The next chapter deals with EFT requirements for this work.

While EFTs offer flexible and adaptable models to explore new physics within known frameworks, GUTs strive for a grand unification of forces at the highest energy scales, attempting to explain fundamental mysteries. Other options in the quest for physics beyond the Standard Model include supersymmetry, string theory, and neutrino physics, each offering distinct perspectives and potential solutions to existing gaps in our understanding of the universe [10].

Effective Field Theory

Observations of physical phenomena in this universe span a vast range of scales, encompassing structures as immense as the universe itself and particles as minuscule as quarks and leptons, which constitute atoms and all matter [11]. Depending on the specific observations, selecting the most appropriate scale becomes imperative in our study of these phenomena. Physics changes according to scale. Effective Field Theory (EFT) emerges as a valuable tool for determining the optimal scale for observing our phenomena. It addresses multi-scale issues, enabling the examination of physical systems across various scales.

EFT provides a means to comprehend the dynamics of a system at low energies without necessitating exhaustive details from much higher energy domains. The formulation of an EFT for any physical system involves adopting one of two standard approaches:

Top-down: In this approach, our understanding of a physical system's behavior at higher energies guides us. By eliminating or integrating out heavier particles or setting a cutoff below these higher energies, we align with a physical system at lower energies through the path integral formalism. Consequently, this approach yields new operators and couplings at these lower energies.

Bottom-up: In contrast, the bottom-up approach lacks knowledge about the physical system at higher energies. Consequently, the Lagrangian is then constructed by considering all the conceivable sets of interactions compatible with the symmetries of the system, employing fields to represent relevant degrees of freedom.

This chapter will delve into the fundamental elements necessary to formulate a low-scale

effective field theory specifically tailored for the described decay process and implying top-down approach. Our primary aim is to comprehensively explore and elucidate all pertinent components essential for constructing the required effective Hamiltonian, both within the confines of the SM and in scenarios that extend beyond its boundaries [12].

The process under our study involves the decay of B_s^0 into its constituent hadrons and is a semi-leptonic decay. All decays of particles involving b quark (and/or b anti-quark) are studies in the regime of B-Physics and specific B-factories are dedicated to this work. The NP hints are hidden in the tree-level and loop-level processes of the decays. Flavour Physics is involved in this study and the mathematical construction and phenomenology of B-Physics are based on the Effective Field Theory.

If there is a high energy scale theory "M" and we want to study the dynamics of the same theory at a lower energy scale "E", then we are going to write the decay amplitude of the required theory in the power of E/M by following processes step by step [3] :

- Start by choosing a cut-off value $\Lambda < M$ and divide the field involved in theory into high and low energy modes

$$\Phi = \Phi_l + \Phi_h$$

  where the low energy modes $\omega < \Lambda$ are contained in Φ_l and the higher frequency Fourier modes $\omega > \Lambda$ are present in Φ_h. Our area of interest is just $\omega < \Lambda$ and even without knowing the physics above this threshold we are quite good to go for our desired theory. In simpler words, even if the structure of the FULL theory is unknown, we can still develop a low-energy effective theory for our desired energy range. The vacuum correlation functions of the field under study (Φ_l) will provide us with all the required information i.e. Feynman Diagrams, scattering cross-sections, decay rates etc. One can acquire these correlators by

$$\langle 0|T\Phi_l(x_1)\dots\Phi_l(x_n)|0\rangle = \frac{1}{Z[0]}\frac{-i\delta}{\delta J_l(x_1)}\cdots\frac{-i\delta}{\delta J_l(x_n)}Z[J_l]|_{J_l=0}$$

  where

$$Z[J_l] \equiv \int \mathcal{D}\Phi_l \mathcal{D}\Phi_h e^{iS(\Phi_l,\Phi_h)+i\int d^D x J_l(x)\Phi_l(x)}$$

is defined as generating functional for our theory. Here

$$S(\Phi_l, \Phi_h) = \int d^D x \mathcal{L}(x)$$

is the action, J_l denotes the low energy modes of fields and D is the space-time dimension representation.

- The higher energy modes of fields can be integrated out simply by integrating over the fields through path integral formalism. The generating functional would then be altered to

$$Z[J_l] = \int \mathcal{D}\Phi_l e^{iS_\Lambda(\Phi_l) + i \int d^D x J_l(x) \Phi_l(x)}$$

  whereas

$$e^{iS_\Lambda(\Phi_l)} = \int \mathcal{D}\Phi_h e^{iS(\Phi_l, \Phi_h)}$$

  is referred as the Wilsonian effective action. This procedure has eliminated the high-frequency mode fields from the functional integral. As a result of excluding these high-frequency fluctuations from the integral, the effective action S_Λ has developed non-local characteristics at scales of $\frac{1}{\Lambda}$.

3.1 Operator Product Expansion

The previously obtained non-local action functional S_Λ can be expressed using local operators through a method known as Operator Product Expansion (OPE). In theoretical physics, particularly in quantum field theory, the Operator Product Expansion (OPE) is a powerful technique used to relate non-local operators to a series of local operators. In this context, the non-local action functional S_Λ, which was derived in the preceding section, captures the physics of a system involving interactions or dynamics at a certain energy scale Λ.

The OPE method allows us to express this non-local action, S_Λ, as a sum or expansion involving a series of local operators. This expansion helps in breaking down the non-local effects into a series of local interactions or observables, providing a more manageable and comprehensible description of the underlying physics. It essentially decomposes the non-local action into a series of simpler local terms, making it easier to analyze and extract information about the system's behavior and properties at different energy scales.

Finally, the action can be written as

$$S_\Lambda(\Phi_l(x)) = \int d^D x \mathcal{L}_\Lambda^{eff}(x)$$

where

$$\mathcal{L}_\Lambda^{eff}(x) = \sum_{i,D} \frac{\mathcal{C}_i^{(D)}}{\mathcal{E}^{D-d}} \mathcal{O}^{(D)}(\Phi_l(x))$$

is defined as the local effective Lagrangian here $\mathcal{C}_i \mathcal{E}^{d-D}$ are called the Wilson coefficients containing short-distance Physics while $\mathcal{O}^{(D)}$ are the operators which encompass long-distance physics.

3.2 Operator Basis for Standard Model Effective Field Theory

The primary benefit of employing an Effective Field Theory (EFT) framework lies in its ability to offer a comprehensively methodical representation of New Physics (NP) effects. This approach facilitates a comprehensive exploration of potential deviations from the Standard Model (SM). When New Physics is hypothesized to possess a weak coupling, the EFT associated with it is often termed the Standard Model Effective Field Theory (SMEFT).

The SMEFT setup is primarily based on all the fundamental fields included within the SM. All terms included in the SM Lagrangian are dimension-four terms. Therefore inclusion of terms for the development of effective theory (in the operator form) higher than four dimensions, requires great care. The operators involved in the construction of weak effective Hamiltonian for the $(B_s^0 \to K_1(1270)(\to \rho(770)\pi)l\bar{\nu}_l$ decay should be gauge invariant (particularly colour singlets) and also Lorentz invariant. This Lorentz invariance implies that fermionic fields should come in the form of pairs. Possible fermionic bilinears in terms of Weyl fields are given as [13]

$$\bar{\psi}_L \gamma^\mu \psi_L, \qquad \bar{\psi}_R \gamma^\mu \psi_R, \qquad \bar{\psi}_L \psi_R, \qquad \bar{\psi}_L \sigma^{\mu\nu} \psi_R, \qquad \bar{\psi}_R \psi_L, \qquad \bar{\psi}_R \sigma^{\mu\nu} \psi_L \qquad (3.2.1)$$

Therefore, the invariant SMEFT operators should satisfy the relation based on baryon and lepton numbers as

$$\frac{1}{2}(\Delta B - \Delta L) \equiv \mathcal{D} \qquad\qquad \text{mod 2.} \qquad (3.2.2)$$

such that $\mathcal{D}$ represents dimension.

We will be working with dim-6 operators and this includes 8 different operator classes $X^3, H^6, H^4D^2, X^2H^2, \psi^2H^3, \psi^2XH, \psi^2H^2D$ and ψ^4, based on the field content. Our class of operators is four-quark dim-6 operators which can be simplified using Fierz identities. The ψ^4 operators are differentiated into multiple groups based on their chiral properties which are listed as:

Dimension-6, $(\bar{L}L)(\bar{L}L)$

The $(\bar{L}L)(\bar{L}L)$ type of operators include

$$Q_{ll} \equiv (\bar{l}_p\gamma_\mu l_r)(\bar{l}_s\gamma^\mu l_t)$$

$$Q_{qq}^{(1)} \equiv (\bar{q}_p\gamma_\mu q_r)(\bar{q}_s\gamma^\mu q_t)$$

$$Q_{qq}^{(3)} \equiv (\bar{q}_p\gamma_\mu\tau^I q_r)(\bar{q}_s\gamma^\mu\tau^I q_t)$$

$$Q_{lq}^{(1)} \equiv (\bar{l}_p\gamma_\mu l_r)(\bar{q}_s\gamma^\mu q_t)$$

$$Q_{lq}^{(3)} \equiv (\bar{l}_p\gamma_\mu\tau^I l_r)(\bar{q}_s\gamma^\mu\tau^I q_t)$$

where the relation of τ^I is given by Fierz identity, p,r,s,t are indices representing flavours and i,j,k,m are weak indices for the SU(2) singlets or SU(2) triplets.

Dimension-6, $(\bar{R}R)(\bar{R}R)$

The $(\bar{R}R)(\bar{R}R)$ type of operators include

$$Q_{ee} \equiv (\bar{e}_p\gamma_\mu e_r)(\bar{e}_s\gamma^\mu e_t)$$

$$Q_{uu} \equiv (\bar{u}_p\gamma_\mu u_r)(\bar{u}_s\gamma^\mu u_t)$$

$$Q_{dd} \equiv (\bar{d}_p\gamma_\mu d_r)(\bar{d}_s\gamma^\mu d_t)$$

$$Q_{eu} \equiv (\bar{e}_p\gamma_\mu e_r)(\bar{u}_s\gamma^\mu u_t)$$

$$Q_{ed} \equiv (\bar{e}_p\gamma_\mu e_r)(\bar{d}_s\gamma^\mu d_t)$$

$$Q_{ud}^{(1)} \equiv (\bar{u}_p\gamma_\mu u_r)(\bar{d}_s\gamma^\mu d_t)$$

$$Q_{ud}^{(8)} \equiv (\bar{u}_p\gamma_\mu T^A u_r)(\bar{d}_s\gamma^\mu T^A d_t)$$

where T^A are the generators of SU(3).

Dimension-6, $(\bar{L}L)(\bar{R}R)$

The $(\bar{L}L)(\bar{R}R)$ type of operators include

$$Q_{le} \equiv (\bar{l}_p\gamma_\mu l_r)(\bar{e}_s\gamma^\mu e_t)$$

$$Q_{lu} \equiv (\bar{l}_p\gamma_\mu l_r)(\bar{u}_s\gamma^\mu u_t)$$

$$Q_{ld} \equiv (\bar{1}_p\gamma_\mu l_r)(\bar{d}_s\gamma^\mu d_t)$$

$$Q_{qe} \equiv (\bar{q}_p\gamma_\mu q_r)(\bar{e}_s\gamma^\mu e_t)$$

$$Q_{qu}^{(1)} \equiv (\bar{q}_p\gamma_\mu q_r)(\bar{u}_s\gamma^\mu u_t)$$

$$Q_{qu}^{(8)} \equiv (\bar{q}_p\gamma_\mu T^A q_r)(\bar{u}_s\gamma^\mu T^A u_t)$$

$$Q_{qd}^{(1)} \equiv (\bar{q}_p\gamma_\mu q_r)(\bar{d}_s\gamma^\mu d_t)$$

$$Q_{qd}^{(8)} \equiv (\bar{q}_p\gamma_\mu T^A q_r)(\bar{u}_s\gamma^\mu T^A u_t)$$

Dimension-6, $(\bar{L}R)(\bar{R}L)$

The $(\bar{L}R)(\bar{R}L)$ type of operators include the hermitian conjugate (h.c.)

$$Q_{ledq} \equiv (\bar{l}_P^j e_r)(\bar{d}_s q_{tj})$$

Dimension-6, $(\bar{L}R)(\bar{L}R)$

The $(\bar{L}R)(\bar{L}R)$ type of operators include the hermitian conjugate (h.c.)

$$Q_{quqd}^{(1)} \equiv (\bar{q}_P^j u_r)\epsilon_{jk}(\bar{q}_s^k d_t)$$

$$Q_{quqd}^{(8)} \equiv (\bar{q}_P^j T^A u_r)\epsilon_{jk}(\bar{q}_s^k T^A d_t)$$

$$Q_{lequ}^{(1)} \equiv (\bar{l}_P^j e_r)\epsilon_{jk}(\bar{q}_s^k u_t)$$

$$Q_{lequ}^{(3)} \equiv (\bar{l}_P^j \sigma_{\mu\nu} e_r)\epsilon_{jk}(\bar{q}_s^k \sigma^{\mu\nu} u_t)$$

The decay under discussion on the quark transition level is a $b \to u$ process. For this very process, the modified operators are mentioned in the next chapter.

3.3 Generalized Structure of Wilson Coefficients

For Wilson coefficients, the general expression can be written as [14]

$$\vec{C}(\mu) = \hat{U}(\mu, M_w)\vec{C}(M_W) \tag{3.3.1}$$

Here $\vec{C}(\mu)$ is a coloumn vector, μ represents the scale that segregates the short-distance (scale $> \mu$) and the long-distance (scale $< \mu$) physics. $\vec{C}(M_W)$ refers to specify the system's starting conditions, which are linked to higher energy scales, specifically characterized by (M_W).

$\hat{U}(\mu, M_W)$ represents a matrix describing how the system evolves or changes over time or different energy scales, with μ signifying a distinct scale or moment in the system's evolution. This matrix encapsulates the transformation or development of the system from its initial state (described by $\vec{C}(M_W)$) to a subsequent state at a different energy scale or moment μ.

The Renormalization Group Equation (RGE) for $\vec{C}(\mu)$ is written as [15]

$$\frac{d}{d(ln\mu)}\vec{C}(\mu) = \gamma^T(g_s)\vec{C}(\mu) \tag{3.3.2}$$

where $\gamma^T g_s$ represents the anomalous dimension matrix of $\mathcal{O}$ operators and it depends on the scale μ given by QCD coupling $\alpha_s(\mu)$. The effective Lagrangian obtained earlier contains an infinite series of operators with mass dimensions D. The same RGE for $\hat{U}(\mu, M_W)$ can be written as,

$$\frac{d}{d(ln\mu)}\hat{U}(\mu, M_W) = \gamma^T g_s \hat{U}(\mu, M_W) \tag{3.3.3}$$

The general solution for this equation is given as

$$\hat{U}(\mu, M_W) = T_g e^{[\int_{g(M_W)}^{g(\mu)}]dg_s \frac{\gamma^T(g_s)}{\beta(g_s)}} \tag{3.3.4}$$

where T_g is said to be the g-ordering operator whereas the function $\beta(g_s)$ serves as a renormalization group function governing the evolution of the coupling constant $\alpha_s(\mu)$. Further $\hat{U}(\mu, M_W)$ sums up the large logarithm $ln(\frac{M_W}{\mu}$ emerging for $\mu << M_W$.

The expansion of ADM $\gamma(\alpha_s)$ using powers of (α_s) and $\beta(\alpha_s)$ using powers of g_s can be formulated in the following manner:

$$\gamma(\alpha_s) = \gamma^{(0)}\frac{\alpha_s}{4\pi} + \gamma^{(1)}(\frac{\alpha_s}{4\pi})^2 + \dots \tag{3.3.5}$$

and

$$\beta(g_s) = -\beta_0 \frac{g_s^3}{16\pi^2} - \beta_1 \frac{g_s^5}{(16\pi^2)^2} - \dots \tag{3.3.6}$$

respectively. Upon substituting Equations 3.3.5 and 3.3.6 into Eq. 3.3.4, we obtain

$$\hat{U}(\mu, M_W) = [1 + \frac{\alpha_s(\mu)}{4\pi}][\frac{\alpha_s(M_W)}{\alpha_s}]^P[1 - \frac{\alpha_s(M_W)}{4\pi}J] \tag{3.3.7}$$

where $J = \frac{P}{\beta_0}\beta_1 - \frac{\gamma^{(1)}}{2\beta_0}$ and $P = \frac{\gamma^{(0)}}{2\beta_0}$

For $C(M_W)$, the expression at NLO can then be written as [16]

$$C(M_W) = 1 + \frac{\alpha_s(M_W)}{4\pi}B \tag{3.3.8}$$

By substituting Equations 3.3.7 and 3.3.8 into Eq. 3.3.1, we obtain an equation for $C(\mu)$ at NLO approximation

$$C(\mu) = [1 + \frac{\alpha_s(\mu)}{4\pi}][\frac{\alpha_s(M_W)}{\alpha_s}]^P[1 + \frac{\alpha_s(M_W)}{4\pi}(B - J)] \tag{3.3.9}$$

This will give us all the NP Wilson Coefficients.

Theoretical Framework of

$B_s^0 \to K_1(1270)(\to \rho(770)\pi)l\bar{\nu}_l$ Decay

This chapter deals with all the necessary details required for the extraction of angular coefficients and physical observables based on them. Utilizing the EFT and a model-independent strategy [17], a complete theoretical framework of the four-fold $(B_s^0 \to K_1(1270)(\to \rho(770)\pi)l\bar{\nu}_l$ decay, then starts with the kinematics part which is the key ingredient to obtain leptonic and hadronic (involving scalar, vector and axial vector-type form factors) amplitudes. Then $K_1 \to \rho$ (cascade part) strong decay is discussed. Afterward, the combined 4-fold amplitude in the form of angular distribution and keeping in view the ρ meson, longitudinal angular coefficients are obtained.

4.1 Helicity Framework of $B_s^0 \to K_1(1270) (\to\rho(770)\pi) l\bar{\nu}_l$ decay

It is of crucial importance to mention that B_s^0 is a heavy meson consisting of a bottom antiquark and a strange quark [18]. K_1 is an axial-vector meson consisting of a strange quark and an up or down antiquark (or vice versa). The physical state of $K_1(1270)$ is a mixture of K_{1A} and K_{1B} states with the mixing angle θ_{K1} which is represented as

$$|K_1(1270)\rangle = |K_{1A}\rangle \sin\theta + |K_{1B}\rangle \cos\theta$$

$\rho(770)$ is a vector meson composed of an up quark and a down antiquark (or vice

versa). The effective Hamiltonian is defined as involving NP scenarios alongside the SM Hamiltonian. NP effects are incorporated through parameterized Wilson Coefficients. The hadronic matrix elements and form factors are provided in this section. Later this section deals with the kinematics required for leptonic and hadronic amplitude calculations.

4.1.1 Effective Hamiltonian

In SM, $b \to ul\nu$ transitions occur at tree-level. We have developed the technology required for studying our exclusive decay channel. The generalized effective Hamiltonian is then written as

$$H_{eff} = \frac{4G_F}{\sqrt{2}} V_{ub} \sum_i \mathcal{C}_i(\mu) \mathcal{O}_i$$

The effective operator basis includes four-fermion operators $\mathcal{O}_i$, where "i" represents V1, V2, S1, S2 and T. These operators exhibit diverse Lorentz and chiral structures, while the corresponding Wilson coefficients are denoted as $\mathcal{C}_i$. These Lorentz and chiral structure of operators is related to spacetime symmetries and left- or right-handedness of particles.

The Lorentz structure of an operator relates to how it transforms under rotations and boosts in spacetime. Chiral structures describe the handedness or helicity of particles in the context of weak interactions. Having different Lorentz and chiral structures implies that these operators represent various possible interactions involving fermions and exhibit different symmetries or transformation properties under rotations and weak interactions.

The effective operators are defined as [19]

$$\mathcal{O}_{V1} = (\bar{u}_L \gamma^\mu b_L)(\bar{\tau}_L \gamma_\mu \nu_L);$$

responsible for left-handed vector currents

$$\mathcal{O}_{V2} = (\bar{u}_R \gamma^\mu b_R)(\bar{\tau}_L \gamma_\mu \nu_L);$$

responsible for right-handed vector currents

$$\mathcal{O}_{S1} = (\bar{u}_L b_R)(\bar{\tau}_R \nu_L);$$

26
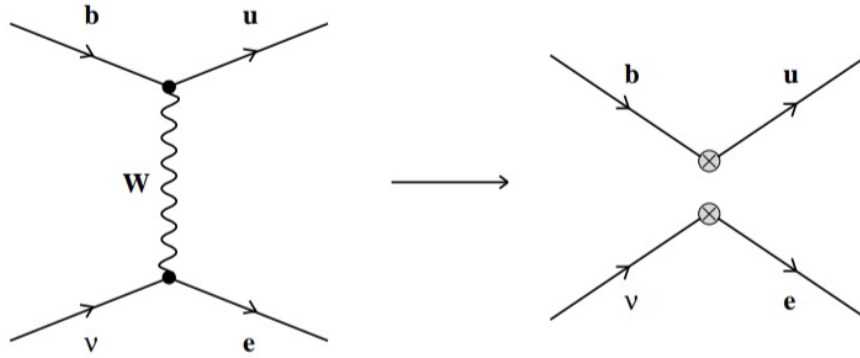
Figure 4.1: An instance of an effective four-fermion interaction derived from integrating the $W^{\pm}$ boson in the Standard Model. The two intersecting circles depicted in the second diagram symbolize a localized four-quark operator within the effective theory [3].

responsible for right-handed scalar currents

$$\mathcal{O}_{S2} = (\bar{u}_R b_L)(\bar{\tau}_R \nu_L);$$

responsible for leftt-handed scalar currents

$$\mathcal{O}_T = (\bar{u}_R \sigma^{\mu\nu} b_L)(\bar{\tau}_R \sigma_{\mu\nu} \nu_L);$$

responsible for tensor type currents

Additionally, the Wilson coefficients $\mathcal{C}_i$ are associated with these operators and represent the coefficients that scale or weight these operators' contributions in a specific physical process or interaction. They quantify the strength of each operator's contribution to a given phenomenon, with each operator having its corresponding Wilson coefficient.

If we consider the neutrinos to have purely left-handed properties, the comprehensive effective Hamiltonian governing the decays involving the transformation of a bottom quark into an up quark along with a charged lepton and a neutrino, encompassing all of the conceivable four-fermion dimension-6 operators that conserve parity, in the Chiral basis of operators, can be expressed as follows:

$$H_{eff} = \frac{4G_F}{\sqrt{2}} V_{ub}[(1 + C_{V1})O_{V1} + C_{V2}O_{V2} + C_{S1}O_{S1} + C_{S2}O_{S2} + C_T O_T] + h.c \quad (4.1.2)$$

Incorporating the operators mentioned above, the above equation takes the form

$$H_{eff} = \frac{4G_F}{\sqrt{2}} V_{ub} [(1 + C_{V1})(\bar{u}_L\gamma_\mu b_L)(\bar{l}_L\gamma^\mu\nu_L) + C_{V2}(\bar{u}_R\gamma_\mu b_R)(\bar{l}_L\gamma^\mu\nu_L)$$

$$+ C_{S1}(\bar{u}_L b_R)(\bar{l}_R\nu_L) + C_{S2}(\bar{u}_R b_L)(\bar{l}_R\nu_L) + C_T(\bar{u}_R\sigma_{\mu\nu}b_L)(\bar{l}_R\sigma^{\mu\nu}\nu_L)] + h.c$$

where G_F is the Fermi coupling constant, V_{ub} is the CKM matrix element for $b \to u$ transition, C_{V1} and C_{V2} are the NP couplings contributing vector and axial vector parts, C_{S1} and C_{S2} are the Wilson coefficients providing scalar and pseudoscalar contributions and C_T contains tensor part. If all these NP contributions are removed, we obtain the Hamiltonian for SM, to which '1' corresponds.

The subscripts 'L' and 'R' represent left and right chiral fields respectively. Explicitly in parity terms, they are written as

$$P_L = \frac{1}{2}(1 - \gamma^5), \qquad\qquad P_R = \frac{1}{2}(1 + \gamma^5)$$

and

$$\sigma^{\mu\nu} = \frac{\iota}{2}[\gamma^\mu, \gamma^\nu]$$

This effective Hamiltonian is sandwiched between initial and final states to obtain the decay amplitude. For a process like $B_s^0 \to M$

$$\mathcal{M} \propto \langle M|H_{eff}|B_s^0\rangle$$

Segregating the effective hadronic and leptonic currents, the 2-fold amplitude for $B_s^0 \to K_1(1270)l\bar{\nu}_l$ reads as

$$\mathcal{M} \propto \langle K_1(1270)|J_{had}^\mu|B_s^0\rangle\langle l\bar{\nu}_l|J_{lep}^\nu|0\rangle \qquad\qquad (4.1.3)$$

4.1.2 Kinematics

This section contains polarization vectors and spinors required for hadronic and leptonic amplitude calculations [20]. In the rest frame of B_s^0, four momenta of B_s^0 is denoted by p^μ, four momenta of axial vector K_1 is denoted by k^μ and q^μ is the momentum transferred to leptons. All four vectors are defined in the contravariant formalism. The

momenta are given as

$$p^\mu = \begin{pmatrix} M_B \\ 0 \\ 0 \\ 0 \end{pmatrix}, \qquad k^\mu = \begin{pmatrix} E_{K1} \\ 0 \\ 0 \\ |q| \end{pmatrix}, \qquad q^\mu = \begin{pmatrix} q_0 \\ 0 \\ 0 \\ -|q| \end{pmatrix}$$

The combined four momenta $(p+k)^\mu$ is written as

$$P^\mu = \begin{pmatrix} M_B + E_{K1} \\ 0 \\ 0 \\ |q| \end{pmatrix}$$

whereas

$$E_{K1} = \frac{(M_B^2 + E_{K1}^2 - q^2)}{2M_B}, \qquad |q| = \frac{\sqrt{\lambda_{BK1}(q^2)}}{2M_B}, \qquad q_0 = \frac{(M_B^2 - E_{K1}^2 + q^2)}{2M_B}$$

and

$$\lambda_{BK1}(q^2) = M_B^2 + M_{K1}^2 + q^4 - 2(M_B^2 M_{K1}^2 + M_B^2 q^2 + M_{K1}^2 q^2)$$

The polarization vectors of K_1 axial vector meson in the rest frame of B_s^0 are defined as

$$\epsilon^\mu(\pm) = \frac{1}{\sqrt{2}} \begin{pmatrix} 0 \\ \mp 1 \\ -\iota \\ 0 \end{pmatrix}, \qquad \epsilon^\mu(0) = \frac{1}{M_{K1}} \begin{pmatrix} |q| \\ 0 \\ 0 \\ E_{K1} \end{pmatrix}$$

The hadronic current polarization vectors (of virtual vector boson η) in the rest frame of B_s^0 are defined as

$$\eta^\mu(\pm) = \frac{1}{\sqrt{2}} \begin{pmatrix} 0 \\ \mp 1 \\ \iota \\ 0 \end{pmatrix}, \quad \eta^\mu(0) = \frac{1}{\sqrt{q^2}} \begin{pmatrix} |q| \\ 0 \\ 0 \\ -q_0 \end{pmatrix}, \quad \eta^\mu(t) = \frac{1}{\sqrt{q^2}} \begin{pmatrix} q_0 \\ 0 \\ 0 \\ -|q| \end{pmatrix}$$

The Dirac spinors, required here, are defined in the chiral basis as

$$u(\lambda = \pm 1/2) = \begin{pmatrix} \sqrt{E \mp |p|}\zeta_\pm \\ \sqrt{E \pm |p|}\zeta_\pm \end{pmatrix}, \qquad \nu(\lambda = \pm 1/2) = \begin{pmatrix} -\sqrt{E \pm |p|}\zeta_\mp \\ \sqrt{E \mp |p|}\zeta_\mp \end{pmatrix}$$

29
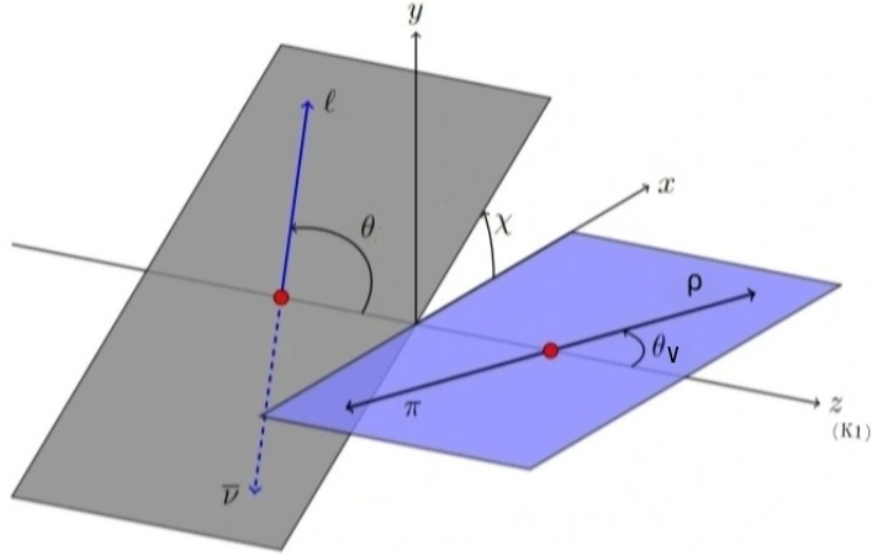
Figure 4.2: Kinematics of $B_s^0 \to K_1(1270)(\to\rho(770)\pi)l\bar{\nu}_l$

such that $\sqrt{E \mp |p|}$ are chirality flipping/conserving factors and helicity eigenspinors are, by definition,

$$\zeta_+ = \begin{pmatrix} \cos\frac{\theta}{2} \\ \sin\frac{\theta}{2}e^{\iota\chi} \end{pmatrix}, \qquad \zeta_- = \begin{pmatrix} -\sin\frac{\theta}{2}e^{-\iota\chi} \\ \cos\frac{\theta}{2} \end{pmatrix}$$

These helicity eigenspinors represent particles of helicity $\pm 1/2$ and antiparticles of helicity $\mp 1/2$; considering neutrinos to be left-handed $\lambda = +1/2$ entirely.

The Dirac matrices in Weyl representation are given as [21]

$$\gamma^\mu = \begin{pmatrix} 0 & \sigma_+^\mu \\ \sigma_-^\mu & 0 \end{pmatrix}$$

and $\sigma_\pm^\mu \equiv (1, \pm\sigma_i)$ such that σ_i portray Pauli matrices.

$$\gamma^5 = \begin{pmatrix} -1 & 0 \\ 0 & 1 \end{pmatrix}$$

Each of these four elements depicts a 2×2 matrix.

4.1.3 Form Factors and Matrix Elements for $B_s^0 \to K_1(1270)l\bar{\nu}_l$ Transition

The inclusive process of semileptonic decay involving B mesons transitioning to daughter $K_1(1270)$ particle alongside their respective leptons and antineutrinos includes calculations of hadronic matrix elements [22]. These transitions can be described and quantified using Lorentz-invariant form factors. The matrix elements are given here by [23]:

$$\langle K_1(k,\epsilon)|\bar{u}b|B_s^0(p)\rangle = -2M_{K1}V_0(q^2)\frac{(\epsilon^*.q)}{M_B + M_u}$$

$$\langle K_1(k,\epsilon)|\bar{u}\gamma^5 b|B_s^0(p)\rangle = 0$$

$$\langle K_1(k,\epsilon)|\bar{u}\gamma^\mu\gamma^5 b|B_s^0(p)\rangle = -\iota\epsilon_{\mu\nu\alpha\beta}\epsilon^{\nu *}p^\alpha k^\beta \frac{2A(q^2)}{M_B + M_{K1}}$$

$$\langle K_1(k,\epsilon)|\bar{u}\gamma^\mu b|B_s^0(p)\rangle = \epsilon_\mu^*(M_B + M_{K1})V_1(q^2) - (p+k)_\mu(\epsilon^*.q)\frac{V_2(q^2)}{(M_B + M_{K1})}$$

$$\langle K_1(k,\epsilon)|\bar{u}\sigma^{\mu\nu}q^\nu\gamma^5 b|B_s^0(p)\rangle = -2\iota T_1(q^2)\epsilon^{\mu\nu\alpha\beta}\epsilon_\nu^* p_\alpha k_\beta$$

$$\langle K_1(k,\epsilon)|\bar{u}\sigma^{\mu\nu}b|B_s^0(p)\rangle = \iota[\epsilon_\mu^*(p+k)_\nu - (p+k)_\mu\epsilon_\nu^*]g_+(q^2)$$
$$+ [\epsilon_\mu^* q_\nu - q_\mu\epsilon_\nu^*]g_-(q^2) + (\epsilon^*.q)[p_\mu k_\nu - k_\mu p_\nu]g_0(q^2)$$

where $\bar{u}b$, $\bar{u}\gamma^5 b$, $\bar{u}\gamma^\mu\gamma^5 b$, $\bar{u}\gamma^\mu b$, $\bar{u}\sigma^{\mu\nu}b$ and $\bar{u}\sigma^{\mu\nu}q^\nu\gamma^5 b$ represent scalar, pseudo-scalar, axial vector, vector and tensor-type hadronic currents respectively and ϵ_μ^* is the polarization vector of K_1 meson.

Another combined relation for the matrix element is given as

$$\langle K_1(k,\epsilon)|\bar{u}\gamma^\mu(1-\gamma^5)b|B_s^0(p)\rangle = \epsilon^{\nu *}[g_{\mu\nu}(M_B + M_{K1})V_1(q^2)$$
$$- (p+k)_\mu q_\nu\frac{V_2(q^2)}{(M_B + M_{K1})} - q_\mu q_\nu\frac{2M_{K1}}{q^2}[V_3(q^2) - V_0(q^2)] + \iota\epsilon_{\mu\nu\alpha\beta}p^\alpha k^\beta\frac{2A(q^2)}{M_B + M_{K1}}$$

The convention used here is $\epsilon_{0123} = 1$ or else on the equivalent footing $\epsilon^{0123} = -1$. $T_1(q^2)$ is the tensor form factor, $g_+(q^2)$, $g_-(q^2)$ and $g_0(q^2)$ relate $T_{1-3}(q^2)$ tensor form factors, $A(q^2)$ represent axial vector form factor, $V_0(q^2)$, $V_1(q^2)$, $V_2(q^2)$ and $V_3(q^2)$ are the vector form factors. The vector form factors are related as

$$V_3(q^2) = V_1(q^2)\frac{(M_B + M_{K1})}{2M_{K1}} - V_2(q^2)\frac{(M_B - M_{K1})}{2M_{K1}}$$

To calculate the physical observables within both the Standard Model (SM) and models of New Physics (NP) across the entire kinematic range, it is essential to parametrize

these form factors. This allows for the estimation of these quantities across the full spectrum of kinematic conditions. For this decay, the calculations of FFs are made in the framework of covariant light-front quark (CLQ) model. The form factors vary based on the square momentum transfer, q², and are subject to extrapolation by the relation

$$F(q^2) = \frac{F(0)}{1 - a(q^2/M_B^2) + b(q^2/M_B^2)^2} \tag{4.1.4}$$

The parametrization in 4.1.4 is used only for the Form Factors (FFs) $V_0(q^2), V_1(q^2)$ and $A_0(q^2)$. For the fitting of $V_2(q^2)$, we need the following parametrization

$$F(q^2) = \frac{F(0)}{(1 - q^2/M_B^2)[1 - a(q^2/M_B^2) + b(q^2/M_B^2)^2]} \tag{4.1.5}$$

Its obvious from these parametrizations that for the maximum recoil condition $q^2 = 0$, the above expressions show

$$F(q^2) = F(0)$$

As K_1 is a mixed state of K_{1A} and K_{1B}, the FFs would be written accordingly. The $q^2 = 0$ numerical values of the $V_0(q^2), V_1(q^2), V_2(q^2)$ and $A_0(q^2)$ are given in Tables 6, 7 and 9 of [23].

4.1.4   Leptonic Amplitudes

The leptonic helicity amplitudes for this decay involve scalar, vector and tensor-type amplitudes. Below they are defined in their respective order

$$L_{S-P}^{\lambda_l}(q^2, \chi, \theta) = \langle l(\lambda_l)\bar{\nu}|\bar{l}(1 - \gamma_5)\nu|0\rangle$$

λ_l is the lepton helicity which is defined in the rest frame of $l\bar{\nu}$. Neutrinos are taken to be massless.

$$L_{V-A,\lambda}^{\lambda_l}(q^2, \chi, \theta) = \eta_\mu(\lambda)\langle l(\lambda_l)\bar{\nu}|\bar{l}\gamma^\mu(1 - \gamma_5)\nu|0\rangle$$

$\eta_\mu(\lambda)$ is the virtual particle's polarization vector defined previously where $\lambda = 0, \pm, t$

$$L_{T-T5,\lambda\lambda'}^{\lambda_l}(q^2, \chi, \theta) = -\iota\eta_\mu(\lambda)\eta_\nu(\lambda')\langle l(\lambda_l)\bar{\nu}|\bar{l}\sigma^{\mu\nu}(1 - \gamma_5)\nu|0\rangle$$

Utilizing the polarization vectors and spinors defined in chiral basis, we obtain all the leptonic components.

The scalar leptonic amplitudes are given as

$$L_{S-P}^+(q^2, \chi, \theta) = -2\sqrt{q^2}\beta e^{-\iota\chi}$$

$$L_{S-P}^-(q^2, \chi, \theta) = 0$$

Expressions of vector leptonic amplitudes read as

$$L_{V-A,+}^+(q^2, \chi, \theta) = -\sqrt{2}m_l\beta \sin\theta e^{-\iota\chi}$$

$$L_{V-A,-}^+(q^2, \chi, \theta) = \sqrt{2}m_l\beta \sin\theta e^{-\iota\chi}$$

$$L_{V-A,0}^+(q^2, \chi, \theta) = 2m_l\beta \cos\theta e^{-\iota\chi}$$

$$L_{V-A,t}^+(q^2, \chi, \theta) = -2m_l\beta e^{-\iota\chi}$$

$$L_{V-A,+}^-(q^2, \chi, \theta) = \sqrt{2q^2}\beta(1 + \cos\theta)e^{-\iota\chi}$$

$$L_{V-A,-}^-(q^2, \chi, \theta) = -\sqrt{2q^2}\beta(1 - \cos\theta)e^{+\iota\chi}$$

$$L_{V-A,0}^-(q^2, \chi, \theta) = -2\sqrt{q^2}\beta \sin\theta$$

$$L_{V-A,t}^-(q^2, \chi, \theta) = 0$$

The explicit formulas for tensor-type amplitudes are

$$L_{T-T5,+0}^+(q^2, \chi, \theta) = \sqrt{2q^2}\beta \sin\theta e^{-2\iota\chi}$$

$$L_{T-T5,-0}^+(q^2, \chi, \theta) = \sqrt{2q^2}\beta \sin\theta$$

$$L_{T-T5,+-}^+(q^2, \chi, \theta) = -L_{T-T5,0t}^+ = 2\sqrt{q^2}\beta \cos\theta e^{-\iota\chi}$$

$$L_{T-T5,+t}^+(q^2, \chi, \theta) = \mp\sqrt{2q^2}\beta \sin\theta e^{-2\iota\chi}$$

$$L_{T-T5,-t}^+(q^2, \chi, \theta) = \mp\sqrt{2q^2}\beta \sin\theta$$

$$L_{T-T5,\pm0}^-(q^2, \chi, \theta) = \pm\sqrt{2}\beta(1 \pm \cos\theta)e^{\mp\iota\chi}$$

$$L_{T-T5,+-}^-(q^2, \chi, \theta) = -L_{T-T5,0t}^- = -2m_l\beta \sin\theta$$

$$L_{T-T5,\pm t}^-(q^2, \chi, \theta) = -\sqrt{2}\beta(1 \pm \cos\theta)e^{\mp\iota\chi}$$

where $\beta = \sqrt{1 - m_l^2/q^2}$

4.1.5 Hadronic Amplitudes

The hadronic current generated as a result of $B_s^0 \to K_1 V^*$ decay has the general amplitude expression as

$$H_{V(A),\lambda}^{\lambda_M}(q^2) = (C_{V(A)} \pm 1)\eta_\mu^*(\lambda)\langle K_1(\lambda_M)|\bar{u}\gamma^\mu(\gamma_5)b|B_s^0(p)\rangle$$

for vector (axial-vector) type currents

$$H_{S(P),\lambda}(q^2) = (C_{S(P)})\langle K_1(\lambda_M = 0)|\bar{u}(\gamma_5)b|B_s^0(p)\rangle$$

for scalar (pseudoscalar) type currents

$$H_{T(T5),\lambda\lambda'}^{\lambda_M}(q^2) = \iota(C_{T(T5)})\eta_\mu^*(\lambda)\eta_\nu^*(\lambda')\langle K_1(\lambda_M)|\bar{u}\sigma^{\mu\nu}(\gamma_5)b|B_s^0(p)\rangle$$

for tensor-type currents

Explicit hadronic currents for scalar, vector and tensor amplitudes are, respectively,

$$H_{S(P),\lambda}(q^2) = \epsilon^*.qE(q^2)$$

$$H_{V(A),\lambda}^{\lambda_M}(q^2) = \epsilon^{\nu*}[g_{\mu\nu}A(q^2) - P_\mu q_\nu B(q^2) - q_\mu q_\nu C(q^2) + \iota D(q^2)\epsilon_{\mu\nu\beta}p^\alpha k^\beta]$$

$$H_{T(T5),\lambda\lambda'}^{\lambda_M}(q^2) = \epsilon^{\nu*}\epsilon^{\mu*}[g_{\mu\nu}F(q^2) - P_\mu q_\nu(G(q^2) + I(q^2)) + q_\mu q_\nu H(q^2) + \iota\epsilon_{\mu\nu\beta}p^\alpha k^\beta J(q^2)]$$

$A(q^2)$ to $J(q^2)$ are the Auxiliary functions which consist of form factors and Wilson coefficients. Auxiliary functions are defined as

$$A(q^2) = (1 + C_{V1} + C_{V2})(M_B + M_{K1})V_1(q^2)$$

$$B(q^2) = (1 + C_{V1} + C_{V2})\frac{V_2(q^2)}{(M_B + M_{K1})}$$

$$C(q^2) = (1 + C_{V1} + C_{V2})\frac{2M_{K1}}{q^2}[V_3(q^2) - V_0(q^2)]$$

$$D(q^2) = (1 + C_{V1} - C_{V2})\frac{2A_0(q^2)}{(M_B + M_{K1})}$$

$$E(q^2) = (C_{S1} + C_{S2})\frac{2M_{K1}}{(M_B + M_u)}V_0(q^2)$$

$$F(q^2) = g_{TL}(M_B^2 - M_{K1}^2)T_2(q^2)$$

$$G(q^2) = g_{TL}T_2(q^2)$$

$$H(q^2) = g_{TL}T_3(q^2)$$

$$I(q^2) = g_{TL}T_3(q^2)\frac{q^2}{(M_B^2 - M_{K1}^2)}$$

$$J(q^2) = 2g_{TL}T_1(q^2)$$

The hadronic amplitudes in helicity basis are given as

$$H_{A,\pm}^{\pm}(q^2) \equiv \mp(C_{V1} - C_{V2} - 1)\frac{\sqrt{\lambda_{BK1}(q^2)}}{M_B + M_{K1}}A_0(q^2)$$

$$H_{V,\pm}^{\pm}(q^2) \equiv -(1 + C_{V1} + C_{V2})(M_B + M_{K1})V_2(q^2)$$

$$H_0(q^2) \equiv H_{V,0}^0 = (1 + C_{V1} + C_{V2})\frac{8(M_B M_{K1})}{\sqrt{q^2}}[V_3(q^2) - V_0(q^2)]$$

$$H_t(q^2) \equiv H_{V,t}^0 = (1 + C_{V1} + C_{V2})\frac{\sqrt{\lambda_{BK1}(q^2)}}{q^2}V_0(q^2)$$

$$H_S(q^2) \equiv -(C_{S1} + C_{S2})\frac{\sqrt{\lambda_{BK1}(q^2)}}{M_B + M_u}V_0(q^2)$$

$$H_{A,0}^0(q^2) = H_{A,t}^0(q^2) = H_P(q^2) = 0$$

All these C's are NP couplings and the SM results can be retrieved by taking them all to be zero. Only V-A structure survives which is the framework of SM.

4.1.6   Cascade Part $K_1 \to \rho\pi$

The axial vector K_1 subsequently cascades to ρ and π mesons; ρ and π are vector and scalar mesons. The parameterization of the decay mode $K_1 \to \rho\pi$ is given by the matrix element, $\langle \rho\pi|K_1(\lambda_M)\rangle$, as [24]

$$\mathcal{A}(K_1(k^\mu) \to \rho(p_v^\mu)\pi(p_s^\mu)) = \frac{-2g_{k_1\rho\pi}}{M_{k1}M_\rho}[(k^\mu.p_{v\mu})(\epsilon_{K_1\mu}(l).\epsilon_\rho^{\mu\dagger}(m)) - (p_v^\mu.\epsilon_{K_1\mu}(l))(k_\mu.\epsilon_\rho^{\mu\dagger}(m))]$$

where $l, m = \pm, 0$ correspond to transverse and longitudinal and polarizations. ϵ_{K_1}, ϵ_ρ and k^μ, p_v^μ represent polarizations and momenta of K_1 and ρ respectively.

In the reference frame of the K_1 meson, the energy and momentum vector of ρ meson are established as

$$\mathcal{E} = \sqrt{M_\rho^2 + |\overrightarrow{P_3}|^2}, \qquad\qquad |\overrightarrow{P_3}| = \frac{\sqrt{\lambda_{K_1\rho\pi}(q^2)}}{2M_{K1}}$$

such that by definition of the Shallon function

$$\lambda_{K_1\rho\pi}(q^2) = M_\rho^2 + M_{K1}^2 + M_\pi^2 - 2(M_\rho^2 M_{K1}^2 + M_\rho^2 M_\pi^2 + M_{K1}^2 M_\pi^2)$$

The momenta mentioned for K_1, ρ and π are explicitly given as

$$k^\mu = (M_{K1}, \overrightarrow{0})$$

$$p_v^\mu = (\mathcal{E}_\rho, |\overrightarrow{P_3}|\sin\theta_V, 0, -|\overrightarrow{P_3}|\cos\theta_V)$$

$$p_s^\mu = (\mathcal{E}_s, -|\overrightarrow{P_3}|\sin\theta_V, 0, |\overrightarrow{P_3}|\cos\theta_V)$$

where $\mathcal{E}_\rho$ and $\mathcal{E}_s$ are the rest mass energies of ρ and π mesons respectively.

In the reference frame of K_1, the polarization vectors of K_1 and ρ mesons are written as

$$\epsilon_{K_1}^\mu(\pm) = \frac{1}{\sqrt{2}}(0, \pm 1, -\iota, 0)$$

$$\epsilon_{K_1}^\mu(0) = \frac{1}{\sqrt{2}}(0, 0, 0, -1)$$

$$\epsilon_v^\mu(\pm) = \frac{1}{\sqrt{2}}(0, \cos\theta_V, \mp\iota, \sin\theta_V)$$

$$\epsilon_v^\mu(0) = \frac{1}{M_\rho}(\overrightarrow{P_3}, \mathcal{E}_\rho\sin\theta_V, 0, -\mathcal{E}_\rho\cos\theta_V)$$

The amplitudes are computed in the K_1 reference frame, where the ρ and π momenta are in the x-z plane. The relative configurations of $\rho\pi$ and $l\bar{\nu}_l$-planes are vividly drawn in Fig: 4.2

4.2   Four Fold Decay; Helicity Amplitudes Formalism

By using the general effective Hamiltonian Sec 4.1.1, One can write the general structure of total helicity amplitude for this process as

$$\mathcal{M}^{TOT} = \mathcal{M}^{SM} + \mathcal{M}^{NP}$$

For the sake of simplicity, the total amplitude does not incorporate leptonic and hadronic tensor parts. The amplitude reads as

$$\mathcal{M} \propto \langle K_1(1270)|J_{had}^\mu|B_s^0\rangle\langle l\bar{\nu}_l|J_{lep}^\nu|0\rangle$$

Considering the virtual boson V^* to be off-shell, the polarization vectors must hold the property

$$\sum_\lambda \eta_\mu^*(\lambda)\eta_\nu(\lambda)\delta_\lambda = g_{\mu\nu}$$

such that

$$\delta_0, \pm = -\delta_t = -1$$

For the $B_s^0 \to K_1 V^*$ process, the general scalar (pseudoscalar amplitude is zero as the corresponding form factor for this decay is zero) and vector (axial vector) amplitudes are given, respectively, as

$$\mathcal{M}_S^{\lambda_l} \propto \langle K_1(\lambda_M = 0)|J_{had}^\mu|B_s^0\rangle\langle l(\lambda_l)\bar{\nu}_l|J_{lep}^\nu|0\rangle = H_S L_S^{\lambda_l}$$

where λ_l is the lepton helicity defined in $l\bar{\nu}_l$ rest frame and λ_M is the helicity of K_1 in the B-frame.

$$\mathcal{M}_{V(A)}^{\lambda_l,\lambda_M} \propto \langle K_1(\lambda_M)|J_{had}^\mu|B_s^0\rangle\langle l(\lambda_l)\bar{\nu}_l|J_{lep}^\nu|0\rangle$$
$$= \sum_\lambda \eta_\mu^*(\lambda)\langle K_1(\lambda_M)|J_{had}^\mu|B_s^0\rangle\eta_\nu(\lambda)\langle l(\lambda_l)\bar{\nu}_l|J_{lep}^\nu|0\rangle\delta_\lambda = \sum_\lambda H_{V(A),\lambda}^{\lambda_M} L_{V-A,\lambda}^{\lambda_l}\delta_\lambda$$

where H and L denote leptonic and hadronic helicity amplitudes.

The total amplitude $\mathcal{M}_{tot}$ for the final state four-body $B_s^0 \to K_1 V^* \to \rho\pi l\bar{\nu}_l$ decay has the generic structure

$$\mathcal{M}_X^{\lambda_l,\lambda_M} \propto \langle K_1(\lambda_M)|J_{had}^X|B_s^0\rangle\langle l(\lambda_l)\bar{\nu}_l|J_{lep,X}|0\rangle \times \langle\rho\pi|K_1(\lambda_M)\rangle BW_{K_1} \qquad (4.2.1)$$

The Breit-Wigner function parameterizes the propagation of the intermediate resonant state which is given for this process as

$$BW_{K_1}(M_{\rho\pi})^2 = \frac{1}{M_{\rho\pi}^2 - M_{K1}^2 + \iota M_{K1}\Gamma_{K1}}$$

The narrow width approximation can be utilized as the width of K_1 is very small $\Gamma_{K1} << M_{K1}$

$$\frac{1}{(M_{\rho\pi}^2 - M_{K1}^2)^2 + M_{K1}^2\Gamma_{K1}^2} \longrightarrow \frac{\pi}{M_{K1}\Gamma_{K1}}\delta(M_{\rho\pi}^2 - M_{K1}^2) \qquad (4.2.2)$$

By keenly looking at the leptonic amplitudes, one can see this relationship between scalar and vector leptonic amplitudes

$$L_S^{\lambda_l} = \frac{\sqrt{q^2}}{m_l}L_{V-A,t}^{\lambda_l} \qquad (4.2.3)$$

Further absorbing scalar hadronic amplitudes H_S into time-like vector hadronic amplitudes $H_{V,t}^0$, we redefine them as

$$\tilde{H}_{V,t}^{\lambda_M(=0)} \equiv H_{V,t}^0 + \frac{\sqrt{q^2}}{m_l}H_S \qquad (4.2.4)$$

37

Utilizing relations mentioned in Eqs 4.2.3, 4.2.4 and summing over the polarizations of vector boson, the generic total amplitude structure in more compact form is given as

$$\mathcal{M}^{\lambda_l,\lambda_M} \propto - \sum_{\lambda=\pm,0} \tilde{H}_\lambda^{\lambda_M,\lambda_l} L_{V-A,\lambda}^{\lambda_l} + \tilde{H}_t^{\lambda_M} L_{V-A,t}^{\lambda_l} \tag{4.2.5}$$

where these redefined amplitudes are as follows [20]

$$\tilde{H}_\pm^{\lambda_M,+} \equiv \tilde{H}_{V,\pm}^{\lambda_M} + \tilde{H}_{A,\pm}^{\lambda_M}$$

$$\tilde{H}_0^{\lambda_M,+} \equiv \tilde{H}_{V,0}^{\lambda_M} + \tilde{H}_{A,0}^{\lambda_M}$$

$$\tilde{H}_\pm^{\lambda_M,-} \equiv \tilde{H}_{V,\pm}^{\lambda_M} + \tilde{H}_{A,\pm}^{\lambda_M}$$

$$\tilde{H}_0^{\lambda_M,-} \equiv \tilde{H}_{V,0}^{\lambda_M} + \tilde{H}_{A,0}^{\lambda_M}$$

$$\tilde{H}_t^{\lambda_M} \equiv \tilde{H}_{V,t}^{\lambda_M} + \tilde{H}_{A,t}^{\lambda_M}$$

The modified hadronic helicity amplitudes with tilde notation are defined as;

$$\tilde{H}_\pm^+(q^2) \equiv H_\pm(q^2)$$

$$\tilde{H}_0^+(q^2) \equiv H_0(q^2)$$

$$\tilde{H}_\pm^-(q^2) \equiv H_\pm(q^2))$$

$$\tilde{H}_0^-(q^2) \equiv H_0(q^2)$$

$$\tilde{H}_t(q^2) \equiv H_t(q^2) + \frac{\sqrt{q^2}}{m_l^2} H_S(q^2)$$

4.3 Four-Body Phase Space

The process under our consideration is a four-body decay, so we need to develop a four-body phase space whose general formula is

$$d^4\Gamma = \frac{|\mathcal{M}|^2}{2m} d\Phi_4 \tag{4.3.1}$$

such that

$$|\mathcal{M}|^2 = \mathcal{M}_{tot}\mathcal{M}_{tot}^\dagger \left(\frac{i}{k^2 - M_{k1}^2}\right)\left(\frac{-i}{k^2 - M_{k1}^2}\right) \tag{4.3.2}$$

where M_{tot} is the four-fold decay amplitude and $M_{tot}^\dagger$ is its complex conjugate whereas $\left(\frac{i}{k^2-M_{k1}^2}\right)$ and $\left(\frac{-i}{k^2-M_{k1}^2}\right)$ represent the corresponding propagator and its conjugate. The four fold decay $B_s^0 \to K_1(\to \rho\pi)l\bar{\nu}_l$ has the decay rate

$$d^4\Gamma = \int \frac{|\mathcal{M}|^2}{2M_B} d\Phi_4(P; P_\rho, P_\pi, P_1, P_2) \tag{4.3.3}$$

The four-body phase space $d\Phi^4$ is given as

$$dLIPS = (2\pi)^4\delta(P - P_\rho - P_\pi - P_1 - P_2) \prod_{i,j=1}^{2} \frac{d^3k_i}{(2\pi)^3 2E_{ki}} \frac{d^3q_j}{(2\pi)^3 2E_{qj}} \tag{4.3.4}$$

$$dLIPS = \frac{dk^2}{2\pi} \frac{dq^2}{2\pi} d\Phi_2(k; P_\rho, P_\pi) d\Phi_2(q; P_1, P_2) d\Phi_2(P; k, q) \tag{4.3.5}$$

where P_ρ, P_π are the four momenta for the cascade decay $K_1(k) \rightarrow \rho(P_\rho)\pi(P_\pi)$ and P_1, P_2 are the momenta for the outgoing final particles generated as a result of vector gauge boson decay; $l(P_1)\bar{\nu}_l(P_2)$ whereas 'P' is the four-momentum vector of the parent particle whose decay looks like this $B_s^0(P) \rightarrow K_1(k)\mathcal{J}^\mu_{eff}(q)$.

The two-body phase space can be generically extended to make a four-fold phase space. Eq.4.3.5 can then be solved by incorporating

$$d\phi_2(k; P_\rho, P_\pi) = \frac{1}{32\pi^2} \frac{\sqrt{\lambda(k^2, P_\rho^2, P_\pi^2)}}{k^2} \int_{-1}^{1} d\cos\theta_V \int_0^{2\pi} d\chi$$

$$d\phi_2(q; P_1, P_2) = \frac{1}{32\pi^2} \frac{\sqrt{\lambda(q^2, P_1^2, P_2^2)}}{q^2} (2\pi) \int_{-1}^{1} d\cos\theta$$

$$d\phi_2(P; k, q) = \frac{1}{32\pi^2} \frac{\sqrt{\lambda(P^2, k^2, q^2)}}{P^2} (2)(2\pi)$$

Where $\lambda(a, b, c) = a^2 + b^2 + c^2 - 2(ab + ac + bc)$. Integrating over the azimuthal and polar angles of the K_1 momentum and the azimuthal angle of the ρ momentum, one obtains

$$d\Phi_4 = \frac{1}{64(2\pi)^6} \frac{\sqrt{\lambda(k^2, P_\rho^2, P_\pi^2)}}{k^2} \frac{\sqrt{\lambda(q^2, P_1^2, P_2^2)}}{q^2} \frac{\sqrt{\lambda(P^2, k^2, q^2)}}{P^2} dk^2 dq^2 d\cos\theta_V d\cos\theta d\chi \tag{4.3.6}$$

Using the Shallon function relations mentioned earlier in Sec 4.1.2 and 4.1.6, the Eq: 4.3.6 becomes

$$d\Phi_4 = \frac{1}{64(2\pi)^6} \frac{|q|}{M_B} \frac{|\vec{P_3}|}{M_{\rho\pi}} (1 - \frac{m_l^2}{q^2}) dq^2 dM_{\rho\pi}^2 d\cos\theta_V d\cos\theta d\chi \tag{4.3.7}$$

4.3.1 The Differential Angular Distribution

Keeping in view the coordinate system as illustrated in Fig: 4.1, the z-axis aligns with the momentum of the K_1 particle in the rest frame of the B_s^0 meson. Furthermore, the x-axis orientation ensures that the momentum of the ρ particle in the rest frame of the K_1 particle lies within the x-z plane and exhibits a positive x-component. The differential angular distribution

$$\frac{d^5\Gamma}{dq^2 dM_{\rho\pi}^2 d\cos\theta_V d\cos\theta d\chi} = \frac{|q|}{256(2\pi)^6 M_B^2} \frac{|\overrightarrow{P_3}|}{M_{\rho\pi}} (1 - \frac{m_l^2}{q^2})|\mathcal{M}|^2$$

After integrating over $M_{\rho\pi}^2$ around the K_1-resonance, for the longitudinally polarized ρ, the distribution above takes the form

$$\frac{d^4\Gamma_\parallel}{dq^2 d\cos\theta_V d\cos\theta d\chi} = \frac{9}{32\pi} N_\parallel I_{\parallel(\perp)}(q^2, \theta_V, \theta, \chi)$$

which can be written explicitly as

$$\frac{d^4\Gamma_\parallel}{dq^2 d\cos\theta_V d\cos\theta d\chi} = \frac{9}{32\pi}[I_{1s,\parallel}\sin^2\theta_V + I_{1c,\parallel}\cos^2\theta_V + (I_{2s,\parallel}\sin^2\theta_V$$

$$+ I_{2c,\parallel}\cos^2\theta_V)\cos 2\theta + (I_{6s,\parallel}\sin^2\theta_V + I_{6c,\parallel}\cos^2\theta_V)\cos\theta + (I_{3,\parallel}\cos 2\chi + I_{9,\parallel}\sin 2\chi)\sin^2\theta_V \sin^2\theta$$

$$+ (I_{4,\parallel}\cos\chi + I_{8,\parallel}\sin\chi)\sin 2\theta_V \sin 2\theta + (I_{5,\parallel}\cos\chi + I_{7,\parallel}\sin\chi)\sin 2\theta_V \sin\theta]$$

where I's are the angular coefficient functions; $I_i \equiv I_i(q^2)$ and $N_\parallel \equiv N_\parallel(q^2)$ such that

$$N_\parallel \equiv N_\parallel(q^2) = \frac{\mathcal{B}(K_1 \to \rho_\parallel \pi)G_F^2|V_{ub}|^2 q^2 \sqrt{\lambda_{BK1}(q^2)}(1 - \frac{m_l^2}{q^2})^2}{48(2\pi)^3 M_B^3}$$

and

$$N_\perp \equiv N_\perp(q^2) = \frac{\mathcal{B}(K_1 \to \rho_\perp \pi)G_F^2|V_{ub}|^2 q^2 \sqrt{\lambda_{BK1}(q^2)}(1 - \frac{m_l^2}{q^2})^2}{48(2\pi)^3 M_B^3}$$

Here $\mathcal{B}(K_1 \to \rho_\perp \pi)$ and $\mathcal{B}(K_1 \to \rho_\parallel \pi)$ are the branching ratios for the cascade decay of transverse and longitudinally polarized ρ. Since the total width is

$$\Gamma(K_1 \to \rho\pi) = \frac{|\overrightarrow{P_3}|}{24\pi M_{K1}^2}(\tilde{\Gamma}_\parallel + \tilde{\Gamma}_\perp)$$

such that

$$\tilde{\Gamma}_\parallel = 2(\frac{-2\lambda_{K_1\rho\pi}}{M_{K1}M_\rho})^2 g_1^2 M_{K1}^2 (M_\rho^2 + |\overrightarrow{P_3}|^2)$$

$$\tilde{\Gamma}_\perp = \frac{M_{K1}^2}{M_\rho^2}[(M_\rho^2 + |\vec{P_3}|^2)g_1 + |\vec{P_3}|^2 g_2]^2$$

where g_1 and g_2 are the couplings

$$g_1 = (\frac{-2\lambda_{K_1\rho\pi}}{M_{K1}M_\rho})$$

$$g_2 = (\frac{2\lambda_{K_1\rho\pi}}{M_{K1}M_\rho})$$

The branching ratios are then given as

$$\mathcal{B}(K_1 \to \rho_\parallel \pi) = \frac{1}{\Gamma(K_1 \to \rho\pi)} \frac{|\vec{P_3}|}{24\pi M_{K1}^2} \tilde{\Gamma}_\parallel$$

$$\mathcal{B}(K_1 \to \rho_\perp \pi) = \frac{1}{\Gamma(K_1 \to \rho\pi)} \frac{|\vec{P_3}|}{24\pi M_{K1}^2} \tilde{\Gamma}_\perp$$

Upon inserting all the numerical values provided in Appendix A, we see that

$\mathcal{B}(K_1 \to \rho_\perp \pi) = 7.14 \times 10^{-1}$ and $\mathcal{B}(K_1 \to \rho_\parallel \pi) = 2.85 \times 10^{-1}$. This implies that $K_1 \to \rho_\perp \pi$ transitions are more probable.

4.4 The Angular Coefficient Functions

The longitudinal angular coefficient functions for $\rho_\parallel$ polarization are given by:

$$I_{1c,\parallel} = 2N_\parallel[|\tilde{H}_0^-|^2 + \frac{m_l^2}{q^2}|\tilde{H}_0^+|^2 + \frac{2m_l^2}{q^2}|\tilde{H}_t|^2]$$

$$I_{1s,\parallel} = \frac{N_\parallel}{2}[3(|\tilde{H}_+^-|^2 + |\tilde{H}_-^-|^2) + \frac{m_l^2}{q^2}(|\tilde{H}_+^+|^2 + |\tilde{H}_-^+|^2)]$$

$$I_{2c,\parallel} = 2N_\parallel[-|\tilde{H}_0^-|^2 + \frac{m_l^2}{q^2}|\tilde{H}_0^+|^2]$$

$$I_{2s,\parallel} = \frac{N_\parallel}{2}[(|\tilde{H}_+^-|^2 + |\tilde{H}_-^-|^2) - \frac{m_l^2}{q^2}(|\tilde{H}_+^+|^2 + |\tilde{H}_-^+|^2)]$$

$$I_{3,\parallel} = -2N_\parallel Re[\tilde{H}_+^- \tilde{H}_-^{-*} - \frac{m_l^2}{q^2}(\tilde{H}_+^+ \tilde{H}_-^{+*})]$$

$$I_{4,\|} = N_{\|} Re[(\tilde{H}_+^- + \tilde{H}_-^-)\tilde{H}_0^{-*} - \frac{m_l^2}{q^2}(\tilde{H}_+^+ + \tilde{H}_-^+)\tilde{H}_0^{+*}]$$

$$I_{5,\|} = 2N_{\|} Re[(\tilde{H}_+^- - \tilde{H}_-^-)\tilde{H}_0^{-*} - \frac{m_l^2}{q^2}(\tilde{H}_+^+ + \tilde{H}_-^+)\tilde{H}_t^*]$$

$$I_{6c,\|} = 8N_{\|} \frac{m_l^2}{q^2} Re[\tilde{H}_0^+ \tilde{H}_t^*]$$

$$I_{6s,\|} = 2N_{\|}[(|\tilde{H}_+^-|^2 - |\tilde{H}_-^-|^2)]$$

$$I_{7,\|} = 2N_{\|} Im[(\tilde{H}_+^- + \tilde{H}_-^-)\tilde{H}_0^{-*} - \frac{m_l^2}{q^2}(\tilde{H}_+^+ - \tilde{H}_-^+)\tilde{H}_t^*]$$

$$I_{8,\|} = N_{\|} Im[(\tilde{H}_+^- - \tilde{H}_-^-)\tilde{H}_0^{-*} - \frac{m_l^2}{q^2}(\tilde{H}_+^+ - \tilde{H}_-^+)\tilde{H}_0^{+*}]$$

$$I_{9,\|} = -2N_{\|} Im[\tilde{H}_+^- \tilde{H}_-^{-*} - \frac{m_l^2}{q^2}(\tilde{H}_+^+ \tilde{H}_-^{+*})]$$

It's essential to note that these angular coefficients not only encompass physical observables but also contain all ascertainable information derived from the analysis of the decay process $B_s^0 \to K_1 \to \rho\pi l\bar{\nu}_l$. The plots of all angular coefficients as a function of q^2 are plotted along with the graphs of other observables in the next chapter. All the aspects of long and short-distance physics within the Standard Model and potential extensions are primarily encapsulated within the angular coefficients. Consequently, these coefficients necessitate the resulting measurements in experimental studies.

Angular Analysis of Observables of $B_s^0 \to K_1(1270)(\to \rho(770)\pi)l\bar{\nu}_l$ Decay and Imprints of NP

This chapter focuses on presenting and discussing the computed physical observables related to the decay $B_s^0 \to K_1(1270)(\to \rho(770)\pi)l\bar{\nu}_l$ within both the SM and the NP scenarios. The initial section includes plots illustrating the angular coefficients $I_i(q^2)$ for longitudinally polarized ρ within the SM and NP scenarios and are thoroughly analyzed. Subsequent sections elaborate on the expressions of physical observables, such as branching ratios (BR), lepton polarization asymmetry (LPA) and the forward-backward asymmetry (FBA), derived in terms of angular coefficients within both the SM and NP scenarios. A detailed discussion and comparison of these aforementioned observables, dissecting their characteristics and differences is presented.

5.1 Phenomenological Analysis of Angular Coefficient (AC) Functions

The parallel angular coefficients previously defined in section 4.4 are discussed in detail. Here we consider the effects on the SM Lagrangian arising from the NP couplings by looking at the individual non-zero value of the Wilson coefficients. The best values for this $b \to u$ decay channel are taken from Table 3 of Reference [25]. Analysis of these observables within SM and in a model-independent framework with separate non-zero

values of NP Wilson coefficients and their combined effect has shown some significant deviations in certain energy ranges from SM. Furthermore, a side-by-side comparison of the results of individual non-zero values of coefficients and their combined effect is also performed. Angular coefficients are plotted as a function of q^2 and their behaviour in different q^2 bins is studied.

The coefficients $I_{1s\parallel}$ (a), $I_{1c\parallel}$ (b), $I_{2s\parallel}$ (c) and $I_{6c\parallel}$ (h) show no deviation from SM in the region [0-8] GeV^2 for values of the NP Wilson coefficients. After these [0-8] GeV^2 energy values a very slight deviation is observed mainly showing C_{V1} contributions. At higher q^2 values NP and SM values again coincide, showing that NP effects are in total agreement with SM results for the whole kinematical region. The plots are provided in Figures 5.1 and 5.2

$I_{2c\parallel}$ (d) indicates negative values and up to the region [0-8] GeV^2, NP results are under SM. An inverted peak obtained around 12 GeV^2 indicates NP sensitivity specifically for C_{V1} as it brings up the change at first order. Other couplings show very minute deviations from SM.

$I_{3\parallel}$ (e) and $I_{4\parallel}$ (f) show extremely small deviations in midway between low and high q^2 values. At starting in the region [0-6] GeV^2 and at the tail end [14-16] GeV^2 all NP scenarios and SM results coincide.

Some Angular Coefficients namely $I_{7\parallel}$ (j), $I_{8\parallel}$ (k) and $I_{9\parallel}$ (l) are considered to be arising from hadronic uncertainties. These coefficient functions arise from imaginary parts of 4-fold helicity amplitude. The NP contributions for these $I_{7\parallel}$ in the region [5-13] GeV^2 and $I_{9\parallel}$ in the region [8-15] GeV^2 are very small. For most of the q^2 values, SM and NP results are in accordance. The case of $I_{8\parallel}$ is very interesting. It shows a very large deviation from SM for right and left-handed vector currents whereas C_{S2} and C_{S1} have overlapping values with SM and do not contribute much to any NP hints. The curve is shifted downwards for C_{V1} contribution and upwards for C_{V2} from SM curve, for the same values of q^2.

$I_{5\parallel}$ (g) is strikingly interesting case because of involved zero crossing. The peaks are shifted above and below the SM value towards a higher q^2 value. This zero crossing is an important indication of the phase transitions. It is the only coefficient
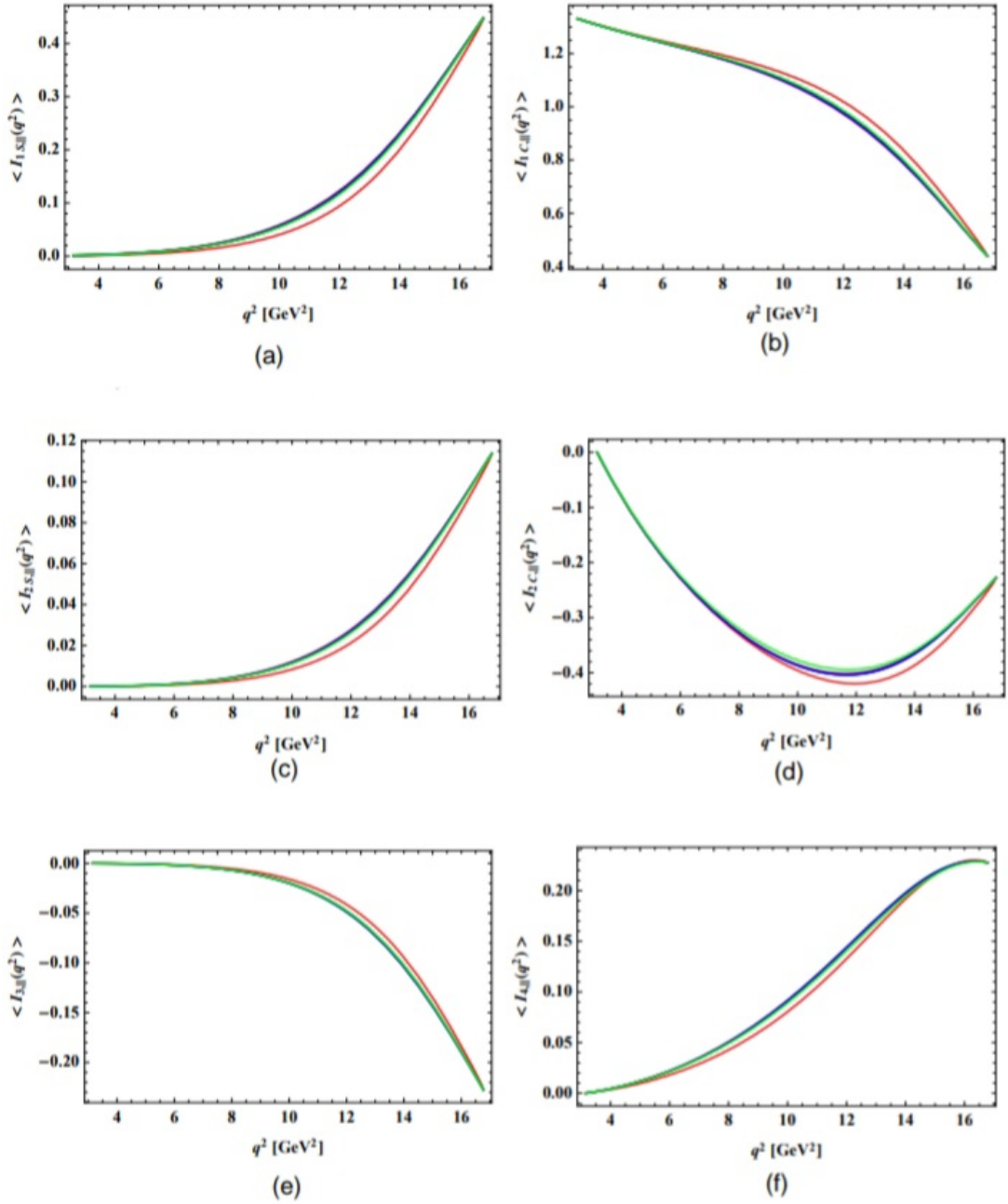
Figure 5.1: Normalized angular observables $I_{1s\parallel}$ (a), $I_{1c\parallel}$ (b), $I_{2s\parallel}$ (c), $I_{2c\parallel}$ (d), $I_{3\parallel}$ (e) and $I_{4\parallel}$ (f) for the decay $B_s^0 \to K_1 \to \rho\pi l\bar{\nu}_l$. Each figure shows the black line for the SM prediction, the red line represents C_{V1} only, the purple line represents C_{V2} only, the blue line represents C_{S1} only and the green line represents C_{S2} only.
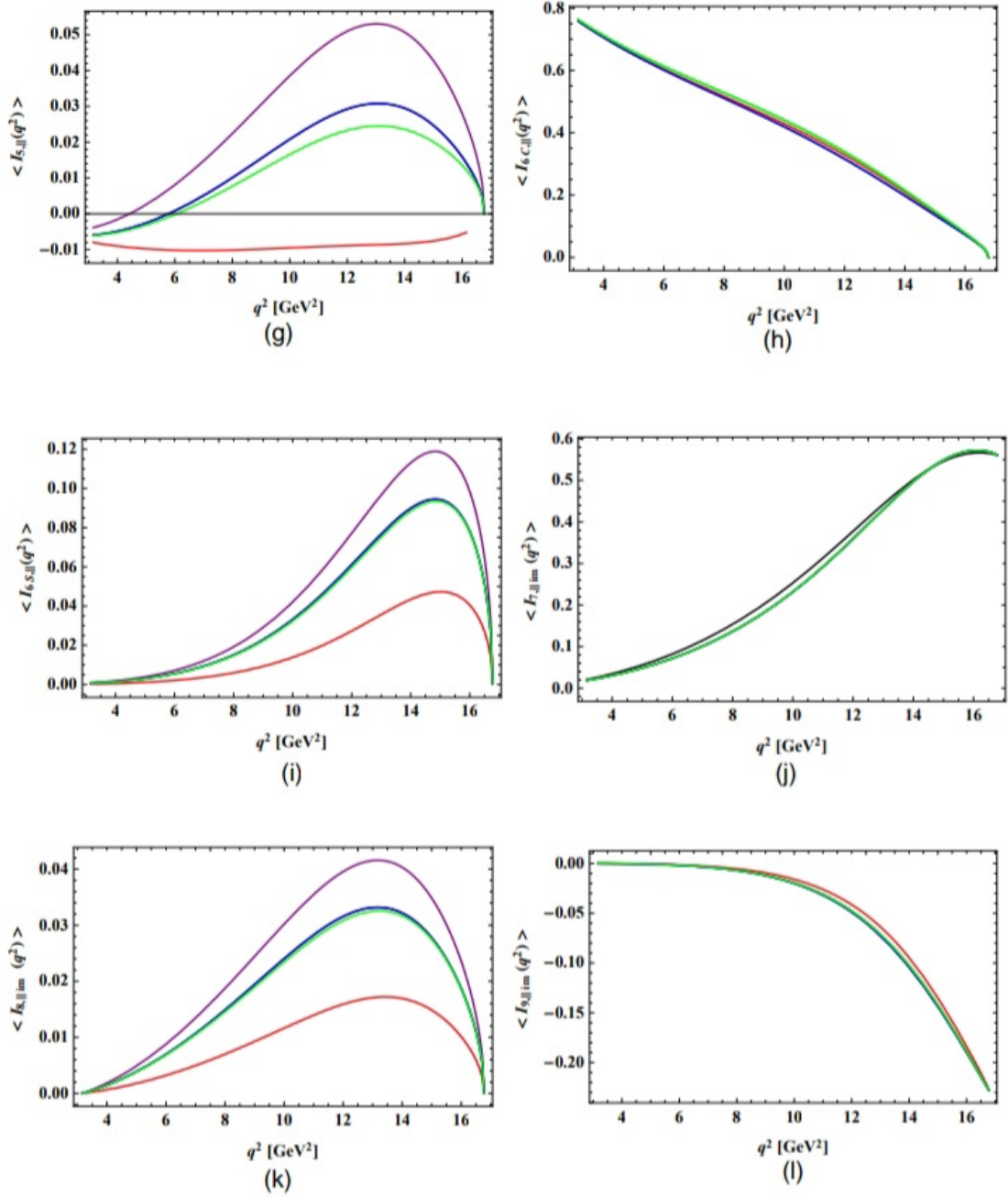
Figure 5.2: Normalized angular observables $I_{5\|}$ (g), $I_{6c\|}$ (h), $I_{6s\|}$ (i), $I_{7\|}$ (j), $I_{8\|}$ (k) and $I_{9\|}$ (l) for the decay $B_s^0 \to K_1 \to \rho\pi l\bar{\nu}_l$. Each figure shows the black line for the SM prediction, the red line represents C_{V1} only, the purple line represents C_{V2} only, the blue line represents C_{S1} only and the green line represents C_{S2} only.

in which scalar current contributions are vividly observable along with vector current contributions. C_{V1} contribution is totally below the zero value indicating an important aspect of the presence of NP. Deviations from the SM predictions might imply the violation of certain symmetries that are assumed to hold in the Standard Model. These could include violations of CP (Charge-Parity) symmetry, flavor symmetries or other fundamental symmetries. Hence $I_{5\parallel}$ should be taken into account while carrying out future experimental studies.

$I_{6s\parallel}$ (i) represents a clear indication of deviation from SM. In this observable C_{V1} has a smaller numerical value than SM results whereas C_{V2} has larger values. However, the peak is shifted towards a higher q^2 value giving us some hint of BSM Physics.

The plots of these angular coefficient observables versus q^2 are plotted in figures 5.1 and 5.2 and their numerical values are provided in Appendix B.

5.2 Physical Observables

The integration of the 4-fold differential decay distribution allows for the construction of various observables using angular coefficients. A few of them are listed here:

5.2.1 Differential Decay Rate

The term "differential decay rate" pertains to how quickly a particle disintegrates into distinct end states within a given phase space or concerning particular parameters. When a particle breaks down into various states or particles, the decay speed can fluctuate based on the specific dynamic characteristics of the resulting particles.

This decay rate is articulated as a mathematical function relying on diverse kinematic variables that delineate the decay mechanism, such as momenta, angles, energies, or other quantifiable factors linked to the decay products. Essentially, it signifies the likelihood per unit phase space or for each unit alteration in these variables that a particle will transform into a specific final state.

We are expressing decay rates in terms of Angular Coefficients. Since we have defined our 4-fold differential decay distribution in terms of angular coefficients which are in

turn defined as the function of the square of momentum transfer;

$$I_i \equiv I(q^2)$$

For the longitudinal polarization of ρ, we obtain the decay rates involving Angular Coefficients as follows:

$$\frac{d\Gamma_{\|}}{dq^2} = \frac{1}{4}(3I_{1c\|} + 6I_{1s\|} - I_{2c\|} - 2I_{2s\|}) \tag{5.2.1}$$

5.2.2 Branching Ratio

The term "branching ratio" or "branching fraction" refers to the ratio of the probability that a specific particle decay channel occurs to the total probability of all possible decay channels for a given particle.

When a particle decays, it can do so through various channels or modes, resulting in different sets of final-state particles. Each decay channel has its own probability associated with it. The branching ratio quantifies the likelihood of a particle to decay through a particular channel compared to all possible decay channels available to it.

Mathematically, the branching ratio BR for a specific decay mode is calculated as the ratio of the partial decay width (Γ_i) of that mode to the total decay width (Γ_{total}) of the particle:

$$BR = \frac{\Gamma_i}{\Gamma_{total}}$$

This provides insight into the dominant decay modes of a particle and helps in understanding the decay processes and the fundamental properties of particles. Measurements of branching ratios in experiments and observations are crucial for verifying theoretical predictions and characterizing the behavior of particles.

To obtain the branching ratio for this four-fold $B_s^0 \to K_1 \to \rho\pi l\bar{\nu}_l$ decay, we simply divide the four-fold differential decay rate Eq. **??** to the total decay width which is defined as $\Gamma_{total} = \frac{h}{2\pi\tau}$, where τ is the life-time of that specific decay mode.

The plot results for Branching Ratio for the longitudinally polarized ρ for the discussed decay are obtained in Fig. 5.3 (a) within SM and NP scenarios. The numerical values are given in Appendix B.

5.2.3 Forward Backward Asymmetry

Forward-backward asymmetry refers to the difference or imbalance observed in the distribution of particle characteristics between the forward and backward directions along the axis of a particle collision or decay. This discrepancy signifies a non-uniform behavior or production of particles in these opposing directions and is crucial for understanding fundamental particle interactions and detecting potential deviations from already established theories.

It is defined as

$$A_{FB} = \frac{N_F - N_B}{N_F + N_B}$$

In this context, N_F represents the count of occurrences where a specific final-state particle moves in the direction designated as "forward" with respect to a specified reference direction and N_B corresponds to the backward direction. The observation of a forward-backward asymmetry in experimental data is significant in providing insights into the underlying symmetries or asymmetries in the fundamental interactions of particles. It serves as an essential aspect of probing the physics beyond the Standard Model of particle physics.

In terms of longitudinal angular coefficient functions, the A_{FB} for this $B_s^0 \to K_1 \to \rho\pi l\bar{\nu}_l$ decay is written as

$$A_{FB,\|}(q^2) = \frac{3}{8}(I_{6c\|} + 2I_{6s\|})$$

Normalized longitudinal A_{FB} is obtained when we divide the $A_{FB,\|}(q^2)$ to $d\Gamma_\|/dq^2$ which is given as

$$< A_{FB,\|}(q^2) >= \frac{3}{8}\frac{(I_{6c\|} + 2I_{6s\|})}{d\Gamma_\|/dq^2}$$

The normalized plots of Forward-Backward Asymmetry are given in Fig. 5.3 (b). For our given kinematical range of q^2, the C_{S1} shows complete coincidence with SM values, however, at higher q^2 values C_{V1} and C_{V2} show large discrepancies from SM whereas a nominal variation from SM for left-handed scalar currents.

5.2.4 Lepton Polarization Asymmetry

Lepton polarization asymmetry refers to the imbalance or discrepancy in the distribution of polarized leptons emitted in different directions, quantified typically by comparing the

number of events or particles with specific spin orientations in the forward and backward directions in a particle interaction or decay process.

The general expression in terms of angular coefficients is given as

$$A_{\lambda_l}(q^2) = \frac{d\Gamma^{\lambda_l=-1/2}/dq^2 - d\Gamma^{\lambda_l=+1/2}/dq^2}{d\Gamma/dq^2}$$

where

$$\frac{d\Gamma^{\lambda_l=-1/2}}{dq^2} = \frac{1}{2}(I_{1c} + 2I_{1s} - I_{2c} + 2I_{2s}) - I_n$$

and

$$\frac{d\Gamma^{\lambda_l=+1/2}}{dq^2} = \frac{1}{2}(I_{1c} + 2I_{1s} + I_{2c} - 6I_{2s}) + I_n$$

Here $\lambda_l = \pm 1/2$ corresponds to the two polarizations of leptons. There is an additional coefficient introduced

$$I_n = 2N\frac{m_l^2}{q^2}|\tilde{H_t}|^2$$

We have not made use of this coefficient beforehand while calculating full angular distribution because previously we summed over lepton polarization states. By the use of longitudinal angular coefficients, we obtained results whose plots are given in Fig. 5.3 (c). The plots represent the asymmetry of polarized leptons emitted in different directions, a zero crossing indicates the point at which the forward and backward directions switch from having a preference for different polarization states (left-handed versus right-handed) to favour the opposite polarization state.

5.2.5 Effect of NP Coefficients for the $B_s^0 \to K_1 \to \rho\pi l\bar{\nu}_l$ Decay Mode

- Effects of $C_{V1} \neq 0$:

By utilizing the best-fit values provided in Appendix A and considering all other NP couplings ($C_{V2} = C_{S1} = C_{S2} = 0$) to be zero, the effects of C_{V1} are studied. The SM results are plotted with a solid black line whereas the C_{V1} contributions are visible with the red line. The branching fractions and forward-backward asymmetry show a very large discrepancy from SM in the C_{V1} scenario. The left-handed vector currents provide significant hints for the NP by imposing constraints on the real and imaginary parts of C_{V1}.
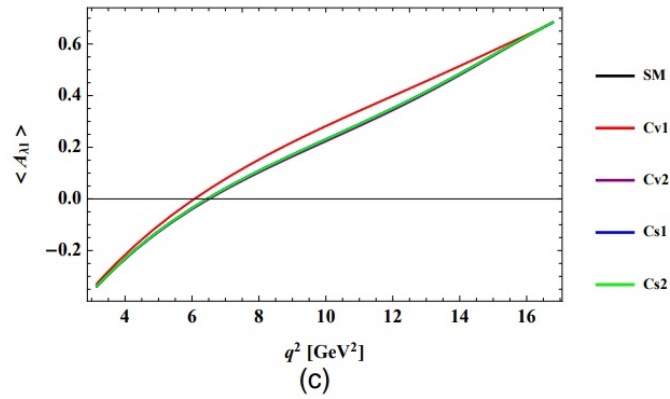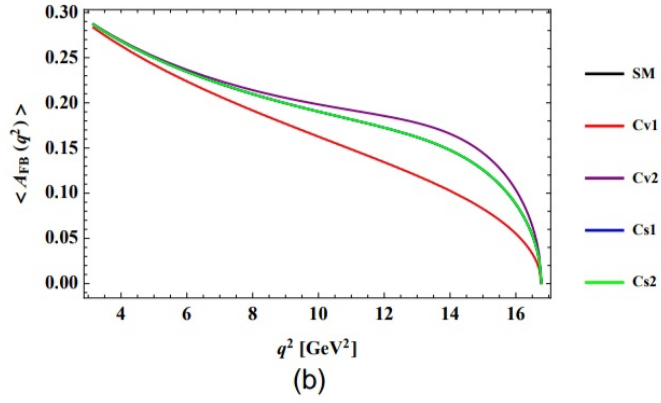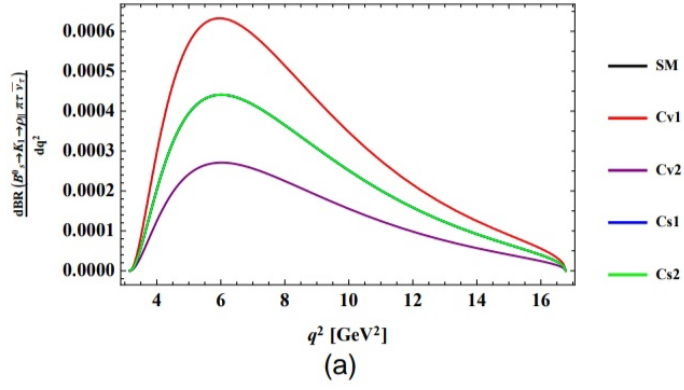
- Effects of $C_{V2} \neq 0$:

(a)

(b)

(c)

Figure 5.3: Branching Ratio (a), Normalized Forward-Backward Asymmetry (b) and Normalized Lepton Polarization Asymmetry (c) for the decay $B_s^0 \to K_1 \to \rho\pi l\bar{\nu}_l$.

By utilizing the best-fit values provided in Appendix A and considering all other NP couplings ($C_{V1} = C_{S1} = C_{S2} = 0$) to be zero, the effects of C_{V2} are studied.The SM results are plotted with a solid black line whereas the C_{V2} contributions are visible with the purple line. The constraint is just applied on the real part of C_{V2}. In branching fractions and forward backward asymmetry the results of purely right-handed vector currents are visible indicating the presence of some underlying phenomenon. The numerical values are either larger (as for branching fraction) or smaller (as in forward-backward asymmetry) than SM predicted values but are always on the opposite to C_{V1} values keeping the SM values as the central ones.

- Effects of $C_{S1} \neq 0$:

By utilizing the best-fit values provided in Appendix A and considering all other NP couplings ($C_{V1} = C_{V2} = C_{S2} = 0$) to be zero, the effects of C_{S1} are studied.The SM results are plotted with a solid black line whereas the C_{S1} contributions are visible with the blue line. In all the physical observables plotted namely branching fractions, forward-backward asymmetry and lepton polarization asymmetry, C_{S1} results are coinciding completely with SM expectation, thereby the left-handed scalar currents are not contributing any new information.

- Effects of $C_{S2} \neq 0$:

By utilizing the best-fit values provided in Appendix A and considering all other NP couplings ($C_{V1} = C_{V2} = C_{S1} = 0$) to be zero, the effects of C_{S2} are studied.The SM results are plotted with a solid black line whereas the C_{S2} contributions are visible with the green line. The non-zero values of NP couplings are clearly distinct from one another, however, the branching fractions, forward-backward asymmetry and lepton spin asymmetry show a very nominal discrepancy from SM in the C_{S2} scenario. No significant deviation from SM values in comparison to C_{S2} coupling is seen. However, the zero crossing point of the lepton spin asymmetry is a considerable point, thereby giving the NP effects solely by the right-handed scalar currents. We also know the energy scale where this asymmetry completely vanishes. The numerical values are provided in Appendix B.

CHAPTER 6

Conclusion

Considering the recent observed deviations in $R_{D(*)}$, $R_{J/\Psi}$ and R_π^l which involve the charged current $b \to cl\nu$ transitions, the $B_s^0 \to K_1(1270) \to \rho(770)\pi l\bar{\nu}_l$ decay has been studied extensively in the model-independent framework. This analysis focused on the semileptonic decay process of the B_s^0 vector meson decaying to an axial vector $K_1(1270)$ meson and a virtual particle which then cascades to a ρ vector meson and a scalar pion coupled with a lepton and its corresponding antineutrino. For this work, only the τ lepton is considered.

The theoretical framework is developed by incorporating Effective Field Theory (EFT). We explored the generalized effective Lagrangian by involving vector and scalar types NP operators. The four-fold amplitude is developed by utilizing the form factors obtained through the framework of the covariant light-front quark model. The four-phase space and full angular distribution have been calculated. We made use of the best-fit values for the NP Wilson coefficients. The effects of these NP parametrizations on angular coefficients and other physical observables have been deeply studied in comparison with SM values. Only the longitudinal polarization ρ vector meson is studied for all the observables.

We provided predictions for multiple observables like BR, FBA and Lepton Polarization Asymmetry which are an important tool for hints at the LFUV. The effects of NP Wilson Coefficients are studied with only one non-zero value at a time. A combined effect of all of them is also studied. According to this study, the following results can be concluded:

- The analysis of the $B_s^0 \to K_1(1270) \to \rho(770)\pi l\bar{\nu}_l$ decay has revealed that the

NP values of most of the angular coefficients coincide with the SM predictions. Except for $I_{8\parallel}$ and $I_{6s\parallel}$ which show very large deviations for left and right-handed vector currents from the SM value. Both of them represent higher values for C_{V2} coupling and lower values of C_{V1} coupling than SM values for the same values of q^2.

- Significant deviations between New Physics scenarios and the Standard Model values in the $I_{5\parallel}$ and the examined physical observable Lepton Polarization Asymmetry. These two have shown zero crossings. Observing the relationship between the zero crossings of different angular observables can reveal information about their phase differences or synchronization.

- The branching ratios have shown significant deviations from SM values indicating the effects of C_{V1} and C_{V2}, where C_{V1} shows much larger values than SM and C_{V2} shows smaller values at the same value of q^2.

- Forward Backward Asymmetry has shown clear deviations from SM for C_{V1} and C_{V2}. However C_{S1} and C_{S2} results coincide with SM predictions. Therefore, NP effects are primarily coming from C_{V1} and C_{V2}.

- C_{S1} and C_{S2} do not contribute much as their deviations from SM are extremely small yet negligible.

- Taking the non-zero values of all the NP couplings collectively shows that the effects arising from C_{V1} and C_{V2} are the most significant ones.

Further precise measurements can be taken by incorporating the theoretical uncertainties arising from hadronic form factors. Therefore, the results vividly indicate the necessity of more experimental data for this decay channel and to better constrain the Wilson Coefficients. Experimental measurements of these observables could result in the exploration of underlying symmetries which are not observed yet.

Appendices

Numerical Inputs

All the numerical input parameters utilized in this study are listed here.

$m_l = m_\tau$	$m_l^2 = q_{min}^2$	M_B	M_{K1}	$(M_B - M_{K1})^2 = q_{max}^2$	M_{pole}
1.777 GeV	3.157 [GeV]^2	5.366 GeV	1.270 GeV	16.7772 [GeV]^2	4.80 GeV

Table A.1: Input values used for numerical analysis

M_ρ	M_π	M_u	G_F	V_{ub}	M_{K1A}	M_{K1B}
0.770 GeV	0.135 GeV	0	$1.15 \times 10^{-5} [GeV]^{-2}$	3.94×10^{-3}	1.31 GeV	1.34 GeV

Table A.2: Further numerical inputs

NP Parameters	New Coefficients	Best-Fit values	1 σ range
C_{V1}	$(\text{Re}[V_L], Im[V_L])$	(0.915, 1.108)	([1.45, 0.65],[1.02, 1.19])
C_{V2}	$(\text{Re}[V_R], Im[V_R])$	(0.116, 0)	([0.205, 0.025],[0.41, 0.41])
C_{S1}	$(\text{Re}[S_L], Im[S_L])$	(0.024, 0)	([0.042, 0.004],[0.092, 0.092])
C_{S2}	$(\text{Re}[S_R], Im[S_R])$	(0.439, 0.005)	([0.457, 0.421],[0.092, 0.092])

Table A.3: The Best-fit values for complex Wilson coefficients used for this $b \to u$ decay

where in the table above Wilson coefficients are defined as

$$C_{V1} = V_L + iV_L \; , \; C_{V2} = V_R + iV_R$$
$$C_{S1} = S_L + iS_L \; , \; C_{S2} = S_R + iS_R$$

Binned Predictions of Angular Coefficients and other Physical Observables

Angular Coefficient	SM	$C_{V1} \neq 0$	$C_{V2} \neq 0$	$C_{S1} \neq 0$	$C_{S2} \neq 0$
$I_{1c,\parallel}$	1.50000	1.500371	1.500385	1.500317	1.5500921
$I_{1s,\parallel}$	0	0	0	0	0
$I_{2c,\parallel}$	0.0000050	0.0000048	0.0000039	0.0000041	0.00000042
$I_{2s,\parallel}$	0	0	0	0	0
$I_{3,\parallel}$	0	0	0	0	0
$I_{4,\parallel}$	0.00080	0.00087	0.00082	0.00088	0.00080
$I_{5,\parallel}$	-0.0098561	-0.0093488	-0.000458	-0.0098257	-0.0098566
$I_{6c,\parallel}$	0.7985476	0.7985441	0.7985423	0.7985467	0.7985496
$I_{6s,\parallel}$	0	0	0	0	0

Table B.1: Average Bin Value Predictions of Normalized Angular Coefficient Functions for this four-fold decay by considering longitudinally polarized ρ in the region $q^2 = (0.0 - 4.0)[GeV]^2$. Standard Model estimation and New Physics scenarios are listed. Errors range of 1σ is considered for new Wilson coefficients.

Angular Coefficient	SM	$C_{V1} \neq 0$	$C_{V2} \neq 0$	$C_{S1} \neq 0$	$C_{S2} \neq 0$
$I_{1c,\parallel}$	1.25264	1.25746	1.25153	1.25265	1.25385
$I_{1s,\parallel}$	0.00739221	0.0047411	0.00800711	0.00739188	0.00728162
$I_{2c,\parallel}$	-0.199657	-0.200424	-0.199479	-0.199648	-0.19667
$I_{2s,\parallel}$	0.000971366	0.000624458	0.00105158	0.000971323	0.000956835
$I_{3,\parallel}$	-0.00158246	-0.00117261	-0.00152949	-0.00158239	-0.00155879
$I_{4,\parallel}$	0.0184133	0.0152756	0.0186858	0.0184124	0.0181378
$I_{5,\parallel}$	-0.000267554	-0.00993153	0.00623248	-0.000270246	-0.00115479
$I_{6c,\parallel}$	0.621003	0.62339	0.620449	0.621035	0.63146
$I_{6s,\parallel}$	0.00486408	0.00185261	0.00623151	0.00486386	0.00479131

Table B.2: Average Bin Value Predictions in the region $q^2 = (4.0 - 7.0)[GeV]^2$.

Angular Coefficient	SM	$C_{V1} \neq 0$	$C_{V2} \neq 0$	$C_{S1} \neq 0$	$C_{S2} \neq 0$
$I_{1c,\parallel}$	1.16542	1.18105	1.16214	1.16543	1.16911
$I_{1s,\parallel}$	0.0295461	0.0204051	0.0314628	0.0295442	0.0288957
$I_{2c,\parallel}$	-0.337598	-0.342126	-0.336649	0.00556396	-0.330167
$I_{2s,\parallel}$	0.00556432	0.003849	0.00592303	-0.337576	0.00544183
$I_{3,\parallel}$	-0.00945803	-0.00732741	-0.00919099	-0.0094574	-0.00924983
$I_{4,\parallel}$	0.0579318	0.0497343	0.0584922	0.057928	0.0566566
$I_{5,\parallel}$	0.0121329	-0.0100003	0.0254928	0.0121245	0.00940058
$I_{6c,\parallel}$	0.49366	0.50028	0.492271	0.493715	0.511619
$I_{6s,\parallel}$	0.0185246	0.00744579	0.0236102	0.0185233	0.0181168

Table B.3: Average Bin Value Predictions in the region $q^2 = (7.0 - 10.0)[GeV]^2$.

58

Angular Coefficient	SM	$C_{V1} \neq 0$	$C_{V2} \neq 0$	$C_{S1} \neq 0$	$C_{S2} \neq 0$
$I_{1c,\parallel}$	1.02102	1.05653	1.01492	1.02104	1.02835
$I_{1s,\parallel}$	0.0969174	0.0752571	0.100638	0.0969106	0.0946405
$I_{2c,\parallel}$	-0.398449	-0.412306	-0.396068	-0.398421	-0.389088
$I_{2s,\parallel}$	0.0215009	0.0167142	0.0223208	0.0214994	0.0209958
$I_{3,\parallel}$	-0.0387424	-0.0324075	-0.0378937	0.125616	-0.0378323
$I_{4,\parallel}$	0.125625	0.114407	0.125884	0.125616	0.122673
$I_{5,\parallel}$	0.0264371	-0.00909804	0.0468301	0.0264206	0.0210499
$I_{6c,\parallel}$	0.351291	0.363509	0.349192	0.35136	0.373593
$I_{6s,\parallel}$	0.0512987	0.0225174	0.0648902	0.0512951	0.0500936

Table B.4: Average Bin Value Predictions in the region $q^2 = (10.0 - 13.0)[GeV]^2$.

Angular Coefficient	SM	$C_{V1} \neq 0$	$C_{V2} \neq 0$	$C_{S1} \neq 0$	$C_{S2} \neq 0$
$I_{1c,\parallel}$	0.75758	0.799573	0.752604	0.757604	0.76559
$I_{1s,\parallel}$	0.249385	0.223022	0.252508	0.249375	0.245916
$I_{2c,\parallel}$	-0.351906	-0.371412	-0.349595	-0.351892	-0.347011
$I_{2s,\parallel}$	0.0604793	0.0541309	0.0612275	0.0604768	0.0596379
$I_{3,\parallel}$	-0.115794	-0.106904	-0.114278	-0.115789	-0.114183
$I_{4,\parallel}$	0.20085	0.196064	0.200228	0.200842	0.198056
$I_{5,\parallel}$	0.0273824	-0.00797897	0.0472528	0.0273662	0.0220474
$I_{6c,\parallel}$	0.182496	0.192611	0.181297	0.182543	0.198083
$I_{6s,\parallel}$	0.0879194	0.0429057	0.110656	0.0879157	0.0866963

Table B.5: Average Bin Value Predictions in the region $q^2 = (13.0 - 16.0)[GeV]^2$.

Physicsal Observable	SM	$C_{V1} \neq 0$	$C_{V2} \neq 0$	$C_{S1} \neq 0$	$C_{S2} \neq 0$
$\frac{dBR_\parallel}{dq^2}$	0.00009998	0.0000999913	0.000099687	0.00009998	0.00009998
$< A_{FB,\parallel}(q^2) >$	0.2798878	0.2798996	0.2798326	0.2798549	0.2798878
$< A_{\lambda_l,\parallel}(q^2) >$	-0.29954	-0.29473	-0.29498	-0.2942632	-0.2948893

Table B.6: Average Bin Value Predictions of the branching ratio, normalized forward-backward asymmetry and normalized lepton polarization asymmetry in the region $q^2 = (0.0 - 4.0)[GeV]^2$. Standard Model estimation and NP Scenarios are listed for the decay channel $B_s^0 \rightarrow K_1(1270)(\rightarrow \rho(770)\pi)l\bar{\nu}_l$.

Physicsal Observable	SM	$C_{V1} \neq 0$	$C_{V2} \neq 0$	$C_{S1} \neq 0$	$C_{S2} \neq 0$
$\frac{dBR_\parallel}{dq^2}$	0.000394369	0.000584977	0.000241062	0.000394388	0.000400578
$< A_{FB,\parallel}(q^2) >$	0.236524	0.235161	0.237342	0.236536	0.240391
$< A_{\lambda_l,\parallel}(q^2) >$	-0.0574657	-0.059903	-0.056901	-0.0575081	-0.0715655

Table B.7: Average Bin Value Predictions in the region $q^2 = (4.0 - 7.0)[GeV]^2$.

Physicsal Observable	SM	$C_{V1} \neq 0$	$C_{V2} \neq 0$	$C_{S1} \neq 0$	$C_{S2} \neq 0$
$\frac{dBR_\parallel}{dq^2}$	0.000334411	0.000492135	0.000204744	0.000334433	0.00034178
$< A_{FB,\parallel}(q^2) >$	0.199016	0.193189	0.202309	0.170231	0.205445
$< A_{\lambda_l,\parallel}(q^2) >$	0.159327	0.152221	0.160815	0.159251	0.133807

Table B.8: Average Bin Value Predictions in the region $q^2 = (7.0 - 10.0)[GeV]^2$.

Physicsal Observable	SM	$C_{V1} \neq 0$	$C_{V2} \neq 0$	$C_{S1} \neq 0$	$C_{S2} \neq 0$
$\frac{dBR_\parallel}{dq^2}$	0.000184105	0.0002658	0.000113066	0.000184119	0.000188621
$< A_{FB,\parallel}(q^2) >$	0.170208	0.153204	0.179615	0.170231	0.177667
$< A_{\lambda_l,\parallel}(q^2) >$	0.345018	0.330666	0.347477	0.344924	0.31342

Table B.9: Average Bin Value Predictions in the region $q^2 = (10.0 - 13.0)[GeV]^2$.

Physicsal Observable	SM	$C_{V1} \neq 0$	$C_{V2} \neq 0$	$C_{S1} \neq 0$	$C_{S2} \neq 0$
$\frac{dBR_\parallel}{dq^2}$	0.0000844938	0.000119266	0.0000519668	0.0000844979	0.0000858852
$< A_{FB,\parallel}(q^2) >$	0.134375	0.104409	0.150978	0.13439	0.139303
$< A_{\lambda_l,\parallel}(q^2) >$	0.526378	0.51121	0.528165	0.526316	0.505145

Table B.10: Average Bin Value Predictions in the region $q^2 = (13.0 - 16.0)[GeV]^2$.

References

[1] https://cds.cern.ch/record/1420264/plots. *CERN Document Server.*

[2] https://physicsworld.com/a/a-triangle-that-matters/. *A triangle that matters, Particles and Interactions.*

[3] Matthias Neubert. Effective field theory and heavy quark physics. *arXiv:0512222 [hep-ph], 1:39*, 2005.

[4] R. Aaij, C. Abellán Beteta, and Ackernley. Observation of enhanced double parton scattering in proton-lead collisions at $\sqrt{s_{NN}} = 8.16$ TeV. *Phys. Rev. Lett.*, 125: 212001, Nov 2020. doi: 10.1103/PhysRevLett.125.212001. URL https://link.aps.org/doi/10.1103/PhysRevLett.125.212001.

[5] Manas K. Mohapatra, N. Rajeev, and Rupak Dutta. Combined analysis of $B_c \to D_s^{(*)}\mu^+\mu^-$ and $B_c \to D_s^{(*)}\nu\bar{\nu}$ decays within Z' and leptoquark new physics models. *Phys. Rev. D*, 105:115022, Jun 2022. doi: 10.1103/PhysRevD.105.115022. URL https://link.aps.org/doi/10.1103/PhysRevD.105.115022.

[6] Paul Langacker. *The Standard Model and Beyond.* CRC Press, 2010.

[7] Mark Thomson. *Modern Particle Physics.* Cambridge University Press, 2013.

[8] Ahmad Ali. Precision tests of the standard model of flavour physics and open issues. December 11 -15, 2023.

[9] Aoife Bharucha Andrzej Buras David Straub Wolfgang Altmannshofer, Patricia Ball and Michael Wick. Symmetries and asymmetries of b → k µ +µ decays in the standard model and beyond. *Journal of High Energy Physics*, 01, 2009.

[10] Andrzej J. Buras. Weak hamiltonian, cp violation and rare decay. *10.48550/ARXIV.HEP-PH/9806471*, 1998.

REFERENCES

[11] Gudrun Hiller and Frank Krüger. More model-independent analysis of → b s processes. *Phys. Rev. D, 69:074020*, Apr 2004. doi: 10.1103/PhysRevD.69.074020. URL https://link.aps.org/doi/10.1103/PhysRevD.69.074020.

[12] Mark B. Wise Aneesh V. Manohar. *Heavy Quark Physics*. Cambridge University Press, 2000.

[13] Aneesh V. Manohar. Introduction to effective field theories. *arXiv:1804.05863v1 [hep-ph]*, 16 Apr 2018.

[14] Andrzej J. Buras and Robert Fleischer. Quark mixing, cp violation and rare decays after the top quark discovery. *arXiv:9704376 [hep-ph], 1:180*, 1997.

[15] Andrzej J. Buras Gerhard Buchalla and Markus E. Lautenbacher. Weak decays beyond leading logarithms. *Rev. Mod. Phys, 68:1125–1244*, 1996.

[16] Andrzej J. Buras. Operator product expansion, renormalization group and weak decays. *arXiv:9901409 [hep-ph], 1:24*, 1999.

[17] Adeva B. et al Aaij. , r. test of lepton universality with b 0 → k 0 + decays. *J. High Energ. Phys. 2017*, August 2017. doi: https://doi.org/10.1007/JHEP08(2017)055.

[18] Ishtiaq Ahmed Zhuo-Ran Huang, Muhammad Ali Paracha and Cai-Dian Lü. Testing leptoquark and z models via b → k1(1270, 1400)µ +µ decays. *Phys. Rev. D, 100:055038*, Sep 2019. doi: 10.1103/PhysRevD.100.05503. URL https://link.aps.org/doi/10.1103/PhysRevD.100.055038.

[19] Hua-Dong Li Cai-Dian Lü Ying-Nan Mao Kingman Cheung, Zhuo-Ran Huang. et al.. revisit to the b → c transition: In and beyond the sm. *Nucl.Phys.B pp.115354. ff10.1016/j.nuclphysb.2021.115354ff. ffhal-02504675f*, 2021.

[20] Ivan Niˇsandˇzic´-Andrey Tayduganov Damir Becirevic, Marco Fedeleb. Lepton flavor universality tests through angular observables of b →d$^{(*)}$lν decay modes. *arXiv:1907.02257v2 [hep-ph]*, 2019.

[21] A.D. Martin K. Hagiwara and M.F. Wade. Exclsive semileptonic b meson decays. *Nuclear Physics B327*, 1989.

[22] Cai-Dian Lü-M. Ali Paracha Faisal Munir Bhutta, Zhuo-Ran Huang and Wenyu Wang. New physics in b → s anomalies and its implications for the complementary

neutral current decays. doi: 10.48550/ARXIV.2009.03588. URL https://arxiv.org/abs/2009.03588.

[23] R C Verma. Decay constants and form factors of s-wave and p-wave mesons in the covariant light-front quark model. *J. Phys. G: Nucl. Part. Phys. 39, 025005*, 2012.

[24] F. Loparco P. Colangelo, F. De Fazio. Probing new physics with $b\text{ß}\rho(770)\nu$ and $b\text{ß}a_1(1260)\nu$, arxiv:1906.07068v2 [hep-ph]. *Phys. Rev. D 100, 075037 (2019)*, 2019.

[25] Rukmani Mohanta1 Atasi Ray1, Suchismita Sahoo. Model independent analysis of $b^* \to pl\bar{\nu}_l$ decay processes. *The European Physical Journal C*, 2019.